Revisiting extreme precipitation amounts over southern South America and implications for the Patagonian Icefields

Tobias Sauter[1]

[1]Climate System Research Group, Institute of Geography, Friedrich-Alexander-University Erlangen-Nürnberg (FAU), Germany

Correspondence to: Tobias Sauter (tobias.sauter@fau.de)

Abstract. Patagonia is thought to be one of the wettest regions on Earth, although available regional precipitation estimates vary considerably. This uncertainty complicates understanding and quantifying the observed environmental changes, such as glacier recession, biodiversity decline in fjord ecosystems and enhanced net primary production. The Patagonian Icefields, for example, are one of the largest contributors to sea-level rise outside the polar regions, and robust hydroclimatic projections are needed to understand and quantify current and future mass changes. The reported projections of precipitation from numerical modelling studies tend to overestimate those from in-situ determinations and the plausibility of these numbers have never been carefully scrutinised, despite the significance of this topic to our understanding of observed environmental changes. Here I use simple physical arguments and a linear model to test the plausibility of the current precipitation estimates and its impact on the Patagonian Icefields. The results show that environmental conditions required to sustain a mean precipitation amount exceeding 6.09±0.64 m yr^{-1} are untenable according to the regional moisture flux. The revised precipitation values imply a significant reduction in surface mass balance of the Patagonian Icefields compared to previously reported values. This yields a new perspective on the response of Patagonia's glaciers to climate change and their sea-level contribution and might also help reduce uncertainties in the change of other precipitation-driven environmental phenomena.

Deleted: The observed dramatic volume loss of the Patagonian Icefields, for example, contradicts the reported positive surface mass balances.

1 Introduction

Patagonia's weather and climate are largely shaped by baroclinic eddies, which are characterized by the interaction of the planetary waves with the mean flow (Garreaud, 2009; Garreaud et al., 2013; Schneider et al., 2003; Vallis et al., 2014). The same mesoscale eddies efficiently transfer water vapor from the tropics poleward (Langhamer et al., 2018a; Schneider et al., 2010; Trenberth et al., 2005), and regularly (every 9-12 days) trigger narrow filaments of water-vapor-rich bursts called atmospheric rivers. These features temporarily increase the vertical integrated water vapor content (IWV) in the Southern Hemisphere mid-latitudes by more than 200% (Durre et al., 2006; Waliser and Guan, 2017). More than half of all extreme precipitation events (above the 98th percentile) in Patagonia are associated with land-falling atmospheric rivers (Waliser and Guan, 2017). Given the tight coupling between atmospheric moisture transport and hydroclimatic response, changes in moisture transport mechanisms not only dominate the inter-annual and multi-decadal precipitation variability in Patagonia (Aravena & Luckman, 2009; Garreaud, 2007; Garreaud & Muñoz, 2005; Muñoz & Garreaud, 2005; Schneider & Gies, 2004;

Viale & Garreaud, 2015; Weidemann et al., 2013; Weidemann et al., 2018), but also dictate the fate of the ice masses in this region.

The Andes constitute an effective barrier to the impinging moist tropospheric air masses, forming one of the most extreme climatic divides found worldwide (Barrett et al., 2009; Garreaud, 2009; Garreaud et al., 2013; Rasmussen et al., 2007; Smith & Evans, 2007). The strong orographic influence on the precipitation distribution is evident from both remote sensing (Wentz et al., 1998) and terrestrial observations (Fig. 1). Despite observational uncertainty along the coast, two characteristic precipitation regions are apparent: (i) a maritime pre-cordillera region with annual precipitation exceeding 2-3 m w.e. (water equivalent), and (ii) a semi-arid rain-shadow region (< 0.5 m w.e.) east of the main ridge that extends several thousand kilometres towards the South Atlantic. However, little is known about precipitation along the main ridge and, in particular, on the Patagonian Icefields. Current estimates from firn cores (Schwikowski et al., 2006; Shiraiwa et al., 2002), discharge measurements (Escobar, 1992) and numerical modelling (Bravo et al., 2019; Lenaerts et al., 2014; Mernild et al., 2017; Schaefer et al., 2013, 2015; Weidemann et al., 2018a) suggest average annual precipitation rates of 5 to 8 m w.e. yr^{-1}, and of 7 to >10 m w.e. yr^{-1} for the Northern and Southern Patagonian Icefield (NPI, SPI), respectively (see Table 1). Extreme precipitation rates between 15 m w.e. yr^{-1} (Mernild et al., 2017; Schaefer et al., 2013, 2015; Schwikowski et al., 2006) and 30 m w.e. yr^{-1} are suspected at isolated locations (Lenaerts et al., 2014). If these precipitation magnitudes are realistic, it is likely that the SPI is one of the wettest – if not *the* wettest – places on earth.

The considerable uncertainty in precipitation amounts in Patagonia not only affects our current understanding of the local hydrological cycle, but also has profound impacts on studies concerned with fjord ecosystems (Landaeta et al., 2012), biological production in water columns (Aracena et al., 2011; Vargas et al., 2018), net primary production (Jobbágy et al., 2002), glacier mass balance (Escobar, 1992; Foresta et al., 2018; Lenaerts et al., 2014; Mernild et al., 2017; Schaefer et al., 2013, 2015; Schwikowski et al., 2006; Shiraiwa et al., 2002; Willis et al., 2012) and its contribution to sea level rise (Malz et al., 2018; Marzeion et al., 2012; Rignot et al., 2003). Reducing the plausible range of precipitation rates is a key step towards improved process understanding of such systems and offers new perspectives on future changes.

Here I use simple physical scaling arguments and a linear modelling approach to test the plausibility of the current precipitation estimates in central Patagonia (45°S-52°S). In particular, I address the question of whether the water vapor flux (WVF) from the tropics to the mid-latitudes by baroclinic eddies can sustain these extreme precipitation estimates. The assessment of the hypothesis relies on three fundamental assumptions: (i) The orographically induced precipitation is proportional to the incoming WVF which acts as the major moisture resource for the precipitation system. This implies that uncertainties in the incoming WVF directly impact the precipitation estimate. (ii) The terrain forced uplift and condensation of moist air masses is assumed to be the dominant precipitation formation process in central Patagonia. (iii) The atmospheric drying ratio (DR) derived from observed isotope data is a valid measure for the cross-mountain fractionation of the WVF. Based on this

Deleted: This criterion requires a stably stratified atmospheric flow, more precisely given by a positive moist buoyancy frequency. During the study period from 2010 to 2016, the condition was fulfilled in more than 99% of all days. As a part of this assumption, the approach also requires a linear mountain flow response, to guarantee that the airflow crosses the mountain range. The linearity requirement was met in 82% of the cases (see Sec. 3.4).

assumption, the proposed methods are constrained by the DR to accurately reproduce the fraction of the water vapor flux removed by orographic precipitation.

After a description of the methods (Sec. 2), the moisture transport in southern South America is explored in more detail (Sec. 3.1). The chapter begins with the analysis of the available atmospheric soundings and compares them with remote sensing products and reanalysis data. Following this, the knowledge gained from the experiments on local precipitation formation (Sec. 3.2) and its implications for the surface mass balance of the SPI (Sec. 3.3) will be discussed and critically reviewed (Section 3.4). The last section provides a conclusion of the main findings.

2 Methodology

DR-scaling

To provide a first assessment of the magnitude of precipitation, mean precipitation is estimated along the western slopes of the Andes (45°-52°S and 73°-76°W) using a simple DR- scaling. The DR in Patagonia, defined as the fraction of the WVF removed by orographic precipitation, is known to be the highest (~0.45-0.5) worldwide (Mayr et al., 2018; Smith and Evans, 2007). The ratio is a characteristic measure for mountain ranges and is independent of the incoming WVF. As the WVF and the DR (here we use 0.45) are known from ERA-Interim data and isotope observations (Dee et al., 2011; Langhamer et al., 2018b; Mayr et al., 2018; Smith and Evans, 2007), one can estimate the mean homogeneous (uniform) precipitation amount. To add altitude-dependent precipitation variability, the amount was redistributed mass-consistently by optimizing the vertical precipitation gradient using a Newton-Raphson algorithm (Press et al., 2007). The precipitation at sea level was taken from the Global Precipitation Measurement (GPM) mission offshore of the Chilean coast (~3 m yr^{-1}). The optimization resulted in a vertical precipitation gradient of ~0.053 % m^{-1}, which represents a slightly higher lapse rate than previously reported rate of ~0.05 % m^{-1} (Schaefer et al., 2013, 2015). This approach converts the entire specified WVF fraction into precipitation regardless of the saturation vapor deficit of the impinging air masses. However, orographic precipitation can only occur when the terrain forced uplift and cooling of air masses lead to water vapor condensation. To take this condition into account, only lower tropospheric (below 950 hPa) air masses are considered with a relative humidity equal to or exceeding 90% (Jarosch et al., 2012; Weidemann et al., 2013). The DR-scaling provides a first-order approximation but neglects heterogeneity and important processes such as airflow dynamics and cloud physics.

Linear orographic precipitation model

To account for these aspects, a set of realistic and extreme ensemble experiments has been designed using a linear orographic precipitation model (OPM), which represents many processes, such as condensation and hydrometeor conversion, using relative simple formulations for airflow dynamics and cloud physics (Garreaud et al., 2016; Jarosch et al., 2012; Smith and Barstad, 2004; Smith and Evans, 2007; Weidemann et al., 2018a). The model builds upon the original formulation of the linear

Formatted: Font: Bold
Deleted: (Mayr et al., 2018; Smith & Evans, 2007).
Field Code Changed
Deleted: (Langhamer et al., 2018; Mayr et al., 2018; Smith & Evans, 2007)…
Deleted: optimizing (Newton-Raphson algorithm)
Deleted: .
Deleted: determined
Deleted: measurements
Deleted: 0.00052 m m^{-1} (
Deleted: 2
Deleted:)
Deleted: smaller
Formatted: Font: Bold

orographic precipitation model (Smith and Barstad, 2004), including a correction of the WVF downstream (Smith and Evans, 2007) and an optimization to enforce the model towards a given drying ratio. It solves two steady-state advection equations describing the condensation of water vapor by terrain forced uplift and conversion from cloud water to hydrometeors. Mountain wave theory allows for the decay of the vertical velocity caused by tilting mountain waves, and consequently constrains the water vapor condensation rate. Assuming horizontal uniform background flow and properties (e.g. atmospheric stability), the orographic precipitation can be represented by a transfer function

Deleted: cold

$$\hat{P}(k,l) = \frac{C_w i\sigma \hat{h}(k,l)}{(1 - imH_w)(1 + i\sigma\tau_c)(1 + i\sigma\tau_f)},$$

with the double Fourier transform of the terrain given by

$$\hat{h}(k,l) = (2\pi)^{-2} \iint h(x,y) e^{-i(kx+ly)} dx\, dy,$$

The spatial pattern of precipitation rate in physical space is obtained from an inverse Fourier transform

Deleted: that can be solved in Fourier space.

$$P(x,y) = max\left[\left(\iint \hat{P}(k,l) e^{i(kx+ly)}\ dk\, dl + P_\infty\right), 0\right],$$

followed by the truncation of negative values. The vertical wavenumber is defined by

$$m(k,l) = \left[\left(\frac{N_m^2 - \sigma^2}{\sigma^2}\right)(k^2 + l^2)\right]^{0.5}$$

where the intrinsic frequency is $\sigma = Uk + Vl$. The parsimonious model contains five parameters, an uplift sensitivity factor C_w, the moist buoyancy frequency N_m^2, the water vapor scale height H_w, and the condensation and fallout time scales τ_c and τ_f. The total precipitation field is obtained by adding up the orographic precipitation from the orographic precipitation model and the background precipitation caused by the synoptic-scale uplift. For consistency, the latter one is calculated by removing the orographic component from the ERA-Interim precipitation field (Dee et al., 2011; Jarosch et al., 2012). To enforce the model towards a given drying ratio DR_{def}, the background precipitation is scaled by a constant, so that the calculated DR corresponds to DR_{def}. The model is solved on a 90 m SRTM dataset, resampled at 1 km resolution (Jarvis et al., 2008). The mean horizontal wind velocities (U, V) and the parameters C_w and N_m^2 are calculated from 6-hourly ERA-Interim fields (2010-2016) below the 500 hPa geopotential level off Patagonia's west coast between 48°-52°S and 75°-78°W (Fig. 1, D1) (Smith

Formatted: Font colour: Red

and Barstad, 2004). On contrary to most other studies, H_w is directly derived from the incoming WVF using $H_w = WVF/(\rho q_w U)$, where q_w is the total mixing ratio and ρ the air density. The time scales of $\tau_c = \tau_f = 850$ s are fixed for all experiments, which are realistic values for Southern Andes and produce remarkable similar results to numerical models (Garreaud et al., 2016; Smith and Evans, 2007).

The orographic precipitation model is used to conduct a suite of ensemble experiments with 40 ensemble members. The ensembles members account for the initial condition uncertainty in the wind direction and moisture content by randomly perturbing $\boldsymbol{U}$ (5%), $\boldsymbol{V}$ (5%), and $\boldsymbol{H_w}$ (10%) around its mean value. In the first experiment, it was tested whether a composite of 'realistic' atmospheric ambient conditions (derived from the reanalysis data), the observed drying ratio of 0.45 (Mayr et al., 2018) and WVF provides the basis to sustain the precipitation estimates of previous studies. The second experiment delivers an 'extreme' scenario by fixing the drying ratio at a higher value of 0.6 and setting the uplift sensitivity factor ($\boldsymbol{C_w = 0.004}$) and moist stability frequency ($\boldsymbol{N_m = 0.007}$) to their 98th percentile values.

Atmospheric Simulations using the Weather Research and Forecast model (WRF)

To analyze the influence of nonlinear flow regimes on precipitation patterns, atmospheric simulations were performed with the Weather Research and Forecast (WRF) model, version 3.8.0. The model was configured with three one-way nested domains with a horizontal resolution of 12.5 km, 2.5 km and 500 m which were centered over the Southern Patagonian Ice Sheet. The model configuration and parameterizations used in this study are shown in Table S4. To achieve the required resolution in the inner domain, the standard terrain data was replaced by NASA Shuttle Radar Topography Mission (SRTM) data (http://www.cgiar-csi.org/data/srtm-90m-digital-elevation-database-v4-1). Furthermore, the land use classification was updated with the ESA CCI data set (https://www.esa-landcover-cci.org). This way the glacier outlines could be improved significantly. The outermost domain was driven at its lateral boundaries by the ERA-Interim reanalysis dataset with a spatial resolution of 0.75° × 0.75° in longitude/latitude and a time interval of 6 hours. With the above setup, individual events were calculated with WRF. Each simulation had a spinup of at least 12 hours.

Deleted: 3

3 Results and Discussion

3.1 Moisture transport

Observations of IWV and WVF are sparse in South America and limits the analysis of the moisture transport to a few locations (see Fig. 2). The only available soundings for the region are Puerto Montt (41.4347°S, 73.0975°W) on the Pacific coast and Punta Arenas (53.0033°S, 70.8450°W) located at the Strait of Magellan (Durre et al., 2006). Along the coast at the latitude of Puerto Montt, the average WVF in the period 1990-2017 was about 165.52±48.51 kg m^{-1} s^{-1}. Land-falling atmospheric rivers temporarily amplify the WVF by more than 400 kg m^{-1} s^{-1}. There is also clear evidence that enhanced atmospheric circulation

Deleted: is

during strong El Niño events (Ocean Niño Index >1.5) increase the moisture flux over several months (see Fig. 2). The El Niño signal is less pronounced in Punta Arenas. The atmospheric soundings show opposite linear long-term WVF trends over the period 1990-2016 with a significant ($p<0.08$) decrease of -4.46 kg m^{-1} s^{-1} (-2.70%) $decade^{-1}$ in Puerto Montt, and a significant ($p<0.05$) positive trend of 8.79 kg m^{-1} s^{-1} (5.11%) $decade^{-1}$ in Punta Arenas (see Fig. 2). However, change-point analysis shows that the observed WVF trend in Punta Arenas is not constant over time, but has shown significant abrupt shifts in the past that characterize the transition of water vapor rich and poor periods (Killick et al., 2012). A significant transition took place in 2006 which marks the beginning of a relative water vapor rich period (Fig. 2).

The ERA-Interim data, on which the analysis is based, reflects the interannual WVF variability and overall trend of the soundings but slightly overestimates the rate of change in Puerto Montt (-4.94 kg m^{-1} s^{-1} $decade^{-1}$, -4.43% $decade^{-1}$), and underestimates the observed trend in Punta Arenas (4.10 kg m^{-1} s^{-1} $decade^{-1}$, 2.70% $decade^{-1}$). The mean WVF at both sites is weaker than the observed moisture transport. In Puerto Montt, the WVF is about 111.54±34.40 kg m^{-1} s^{-1}, which is almost 30% less than the estimate from the atmospheric sounding. The differences between observed WVF (172.12±54.19 kg m^{-1} s^{-1}) and reanalysis data (152.08±57.08 kg m^{-1} s^{-1}) is much lower in Punta Arenas. It is evident from the soundings that ERA-Interim data is too dry (according to the IWV) in the vicinity of Puerto Montt (-2.23 mm, -14.9%, $p<0.01$), and slightly too wet in the south (0.48 mm, 4.6%, $p<0.05$) (see Fig. S2 and Table S2). The comparison with atmospheric water vapor data obtained by the Special Sensor Microwave Imager/Sounder (SSMIS) over the ocean confirms the north-south pattern (Wentz et al., 1998) (see supporting information Fig. S4). While IWV differences between ERA-Interim data and SSMIS south of 45°S are on average smaller than 0.16 mm (1.1%), larger deficits are apparent north of 45°S (<-0.8 mm).
Based on the comparison with the atmospheric soundings and SSMIS observation, ERA-Interim underestimates the IWV along the west coast of Patagonia (D1 in Fig. 1), where the corresponding parameters for the assessment were calculated, by less than 5%. However, comparison with the soundings suggests that the WVF in the ERA-Interim data along the west coast is weaker by 10-20% due to uncertainties in moisture advection. In the following analysis, a WVF bias of 10% is assumed and corrected accordingly.

3.2 Physical constraints on local precipitation

To obtain the plausible range of precipitation amounts in central Patagonia, the DR-scaling and the linear model are driven by the ERA-Interim data for the period 2010-2016. The DR-scaling results in a mean precipitation rate of 3.45±0.14 m yr^{-1} in the Pre-Cordillera region, with maximum values of 4.89±0.97 m yr^{-1} (see Fig. 1). Averaged over the SPI and NPI, this approach produces values of 5.46±1.30 m yr^{-1} and 5.38±1.26 m yr^{-1}, respectively (Table 1). The highest peaks on the icefields receive precipitation amounts of up to 9.63±3.69 m yr^{-1}.

The orographic precipitation model is applied to a large domain (Fig. 1, D2) to avoid spurious numerical artefacts. The ensemble mean of the realistic experiment (DR=0.45) gives an average precipitation amount of 5.06±0.51 m yr^{-1} over the SPI

Deleted: SSMIS

Deleted: data

Formatted: Font colour: Red

Deleted: 2

and 5.38±0.59 m yr^{-1} over the NPI (Table 1, Fig. 3), indicating that the WVF can sustain relatively high mean precipitation amounts in Patagonia. However, precipitation estimates are up to 38% lower than estimates from previous numerical studies (Escobar, 1992; Lenaerts et al., 2014; Mernild et al., 2017; Schaefer et al., 2013, 2015; Schwikowski et al., 2006). The highest mean amounts are found on the western slopes of the icefields (5.93±0.60 m yr^{-1}) and at the southernmost end of the SPI. The eastern slopes receive considerably less precipitation (4.04±0.42 m yr^{-1}). Comparison with in-situ observations from the Dirección General de Aguas (DGA, Chile) indicates that the model slightly overestimates precipitation on the leeward side by 0.29±0.37 m yr^{-1} (see Table S3). Higher deviations (1.07±1.30 m yr^{-1}) occur at the stations on the west side which are located at the foot of the Patagonian Icefields. The overestimation is the result of the rapid increase in model terrain elevation and the absence of nonlinear processes in the linear model (see Sec. 3.4). The maximum precipitation amount (10.09±0.92 m yr^{-1}), found on the SPI plateau, is ~30-70% lower than previously simulated extremes (Lenaerts et al., 2014; Schaefer et al., 2013, 2015) and accumulation rates derived from an ice core (Shiraiwa et al., 2002). The large ensemble spread indicates that extreme precipitation is very sensitive to small uncertainties in ambient flow conditions (see Table 1). Even though the uncertainty in the background flow regime and dynamics may also be a possible origin of the extreme precipitation predicted by the mesoscale models, the responsible mechanisms explaining the significant differences remain unclear. It is likely that one reason is the model parameterization of processes. Some microphysical parameterization schemes are more ‘graupel-friendly’ than others, which can lead to strong hydrometeor formation. Since the choice of parameterization combinations can lead to very different results, each model must be examined individually. The sources are manifold and can only be speculative in the context of this study.

The extreme experiment shows higher averaged precipitation amounts of 5.99±0.59 m yr^{-1} and 6.09±0.64 m yr^{-1} at the SPI and NPI, respectively (Fig. 3). The combination of short time scales, large drying ratio, strong moist stability frequency, and large uplift sensitivity factor increases the total precipitation and enhances the cross-mountain fractionation. Despite the precipitation-enhancing parameter choices, the maximum precipitation (11.58±0.98 m yr^{-1}) represents a reduction of up to 60% compared to other numerical studies (Lenaerts et al., 2014; Schaefer et al., 2013, 2015). In addition, the estimated maximum is presumably an overestimate itself, due to the ‘extreme’ parameter choice and to the exclusion of nonlinear effects, such as flow blocking (see Sec. 3.4), given the linear nature of the orographic model.

3.3 Consequences of revised precipitation estimates on the surface mass balance of the SPI

These revised precipitation estimates have critical implications for our current understanding of the response of Patagonia’s glaciers to climate change. Recent numerical studies (Mernild et al., 2017; Schaefer et al., 2015) suggest a mean annual surface mass gain of 1.78±0.36 m to 2.24 m w.e. yr^{-1} for the SPI over recent decades, while surface mass balance (SMB) estimates for the NPI range between -0.16±0.73 m w.e. yr^{-1} and 0.14±0.49 m w.e. yr^{-1}. However, these assessments used mean precipitation rates well above (40-65%) the plausible range presented in this study.

Deleted: While these values agree with

Deleted: derived from water discharge measurements (Escobar, 1992) and ice core stable isotopes records (Schwikowski et al., 2006), they

Field Code Changed

Deleted: windward side

Deleted: 6.95±0.70

Deleted: leeward

Deleted: The spatial pattern on the plateau is consistent with the observed elevation gain from radar interferometric measurements (Malz et al., 2018).

Deleted: de

Deleted: 2

Deleted: Greater

To quantify the effect of the revised precipitation values on the SMB, we use the significant linear relation (R^2=0.96, $p<0.05$) between precipitation sum and annual SMB derived from Schaefer et al. (2015) (see Fig. 4), given by SMB=1.2588·P_S-3.9355, where P_S is the mean solid precipitation. Taking into account the proposed solid to total precipitation ratio of 0.596 (Schaefer et al., 2015), the mean solid precipitation is 3.02±0.30 m w.e. (realistic scenario) and 3.57±0.35 m. w.e. (extreme scenario) for the SPI. Based on this assumption, the revised accumulation values would result in a mean SMB between 0.56±0.45 m w.e. yr^{-1} (7.82±6.28 km^{-3} yr^{-1}, extreme scenario) and -0.14±0.39 m w.e. yr^{-1} (-1.95±5.45 km^{-3} yr^{-1}, realistic scenario) on the SPI (Fig. 4). The SMB estimate from the DR-scaling is within these limits. Taking account of the recent geodetic mass balance observations (-0.941±0.19 m w.e.) (Malz et al., 2018), the mean mass loss due to calving ranges between -1.5±0.64 (-20.95±8.94 km^{-3} yr^{-1}) and -0.8±0.58 m. w.e. yr^{-1} (-11.18±8.10 km^{-3} yr^{-1}). The mean mass balance and calving flows derived here are subject to approach-related uncertainties and may deviate strongly from the values of individual years. A recently published study showed that calving fluxes at Jorge Montt Glacier fluctuated between 1.16±0.66 km^{-3} yr^{-1} and 3.81±1.10 km^{-3} yr^{-1} in the years 2012-2018 (Bown et al., 2019). Single events cannot be represented with the approach presented here, since the mean SMB is used together with the geodetic mass balance observations which also constitutes an integrated value. Furthermore, an invariant and homogeneous liquid to solid precipitation ratio and a universal relationship between annual precipitation sums and SMB is assumed. Recently published studies indicate that the solid to liquid precipitation ratio vary locally (Bravo et al., 2019). Together with the snowdrift effect, which is not considered here, this leads to large uncertainties in the mass change estimates. However, this analysis clearly shows how sensitive the estimation of SMB and calving rates react to precipitation uncertainties.

Deleted: (

Moved (insertion) [1]

Deleted: ,

Deleted: (Schaefer et al., 2013, 2015)

Deleted: . (see Fig. 4), which follows

Moved up [1]: (Schaefer et al., 2013, 2015).

Deleted: The SMB and calving flux might be even smaller when considering snowdrift effects.

Deleted: ¶

Given the strong link between glacier SMB and the local hydrological cycle, the long-term SMB evolution scales with the strength of the WVF, which is, in turn projected to increase in a warming climate. The WVF sensitivity along Patagonia's west coast (~50°S) is on the order of ~15% K^{-1} (~3% $decade^{-1}$) as a result of the strengthening of the westerlies (~20% K^{-1}) and increase in IWV (~5% K^{-1}) south of 45°S. The latter is weaker than the change in global-mean IWV which scales according to the Clausius-Clapeyron relation (7% K^{-1}) but is consistent with the assumption that increased latent heat flux is compensated by the sensible heat flux (Held et al., 2006; Schneider et al., 2010). The observed zonal wind trend is associated with a bias towards a more positive Southern Annular Mode (Garreaud et al., 2013; Marshall et al., 2017; Thompson & Solomon, 2002). The change of the WVF leads to stronger moisture flux convergence along the coastal zone west of the Andes main ridge. Ignoring the fact that the solid-liquid ratio changes, which appears to be a reasonable assumption since temperature changes in the lower troposphere are negligible (~0.01 K dec^{-1}), a mean mass gain of 0.57±0.06 m w.e. per degree warming (0.11±0.02 m w.e. $decade^{-1}$) is expected over the SPI. This rate is consistent with other studies (Mernild et al., 2017). Thus, although the precipitation values presented here indicate that present-day SMB of the SPI is likely not as positive as suggested by previous studies, SMB can be expected to show an increasing trend under continued warming conditions.

Deleted: Antarctic

Deleted: a

Deleted: m

3.4 Limitations and nonlinearities

Given the linear nature of the approach used, the knowledge gained must be critically assessed and is only valid under certain conditions. This linear assumption requires a stably stratified atmospheric flow, more precisely given by a positive moist buoyancy frequency. During the study period from 2010 to 2016, the condition was fulfilled in more than 99% of all days. As a part of this assumption a linear mountain flow response is required, to guarantee that the airflow crosses the mountain range. To ensure a linear flow regime, the non-dimensional mountain height $\bar{H} = (N_m\, h_m)/U$ must be smaller than one, where h_m is the mean barrier height. Assuming a mean $h_m = 2200$ m, the conditions ($\bar{H} < 1$) is fulfilled in >82% of all considered cases (see Fig. S5). In the remaining cases ($\bar{H} \geq 1$), the Andes block the atmospheric flow, and a northerly low-level barrier jet forms along the west slope, parallel to the main ridge (Barrett et al., 2009; Falvey and Garreaud, 2007; Garreaud and Muñoz, 2005; Viale and Garreaud, 2015) (see Fig. 5). The low-level jet constitutes an effective barrier to the flow that extends upwind, greatly reducing the uplift motions and thus the condensation of water vapor along the west slopes. The shift in the vertical uplift enhances precipitation upstream of the Andes, while reducing precipitation at the slopes. The effect of blocking is clearly evident in the precipitation fields of high-resolution (500 m) atmospheric simulations of single events using the Weather Research and Forecast (WRF) model (see Fig. 6 and Table S4). Two water-vapor-rich events were chosen to illustrate the influence of the flow regime on the spatial distribution of precipitation. While the linear flow regime has a pronounced precipitation maximum on the slopes, flow blocking shifts the precipitation far upstream (600-700 km) leading to a more homogeneous pattern.

Deleted: In view of

Deleted: A necessary requirement is the

Deleted: 6

Deleted: 7

Deleted: 3

Deleted: ¶

Upstream precipitation can be further enhanced by microphysical processes such as the seeder-feeder mechanism and rapid warm air autoconversion. Studies have shown that these processes can lead to higher rain accumulations upstream when fronts and embedded atmospheric rivers intersect the west coast of central Chile (Garreaud et al., 2016; Massmann et al., 2017; Viale et al., 2013; Viale and Garreaud, 2015). The lifting of moist air masses upstream produces mid-tropospheric stratiform clouds (seeder) which can be strong enough to produce snow/graupel aloft and light precipitation in the pre-frontal region. If the frontal system is slowed down by blocking, low-level convergence enhances in the area of the narrow cold-frontal rainband and fuels the updrafts. The enhanced updrafts facilitate the development of low-level clouds by collision-coalescence between supercooled droplets. When the narrow cold frontal rainband propagates further east it triggers the seeder-feeder mechanism and low-tropospheric clouds are seeded by the precipitation that is formed by mid-tropospheric clouds aloft. The associated rapid transformation of cloud water into hydrometeors and increased hydrometeor sizes are absent in the approach presented. Here, the process is treated simplistic by the choice of small time scales and by constraining the synoptic-scale uplift (background precipitation). This solution most likely lead to (i) an overestimation of precipitation on the west slopes of the SPI, (ii) an underestimation of precipitation in the Pre-Cordillera zone, but (iii) satisfies the given DR_{def} constraint. Compliance with the DR criterion is the necessary condition to verify the plausibility of precipitation estimates.

4 Conclusion

The present study has shown on the basis of simple physical arguments and a linear model that it is very unlikely that the moisture flux from the Pacific will be sufficient to sustain the reported extreme mean precipitation amounts for Patagonia. While the approaches and assumptions employed in this study contain substantial uncertainties, precipitation estimates using other parameter combinations fall within the range between the realistic and the extreme scenario. Hence, this study offers a plausible range of precipitation estimates based on clearly defined assumptions: (i) the orographically induced precipitation is proportional to the incoming WVF, (ii) the terrain forced uplift and condensation of moist air masses is assumed to be the dominant precipitation formation process in central Patagonia, and (iii) the atmospheric drying ratio (DR) derived from observed isotope data is a valid measure for the cross-mountain fractionation of the WVF. The values within this range are about 40-65% lower than previously assumed. Extreme precipitation in wind-exposed regions is in the range of 11.58±0.98 m yr^{-1}, up to 60% lower than estimated by other numerical studies (Lenaerts et al., 2014; Schaefer et al., 2013, 2015). It should also be noted that processes such as snowdrift and nonlinear effects have not been taken into account so that the actual accumulation rates are probably still below these estimates. This result makes it very unlikely that Patagonia is the wettest place on Earth. More importantly, the drier hydroclimatic condition represents a major constraint for the Patagonian Icefields and reduces the precipitation contribution to the glacier mass balance. The missing contribution is evident in the surface mass balance. According to the results, the average SMB was between 0.56±0.45 m w.e. yr^{-1} (7.82±6.28 km^{-3} yr^{-1}) and -0.14±0.39 m w.e. yr^{-1} (-1.95±5.45 km^{-3} yr^{-1}) in the last decades. On the long-term, the regional precipitation is likely to increase by ~15% per degree warming in response to stronger moisture flux. Assuming that the liquid to solid precipitation ratio and the relationship between annual precipitation sum and SMB are universal and valid for the next decades, the WVF changes would result in a glacier surface mass gain of about 0.57±0.06 m w.e. per degree warming. This positive trend contradicts the recently published geodetic mass balance observations (Malz et al., 2018), which detected quick glacier recessions in these regions. The observed retreat is significantly stronger than the gain in ice mass implying that the ice mass budget is partially decoupled from the climate signal and primarily caused by dynamic adjustments of tidewater and lake calving glaciers. The pronounced dynamic glacier response emphasizes that ice dynamic processes need to be given more prominence in order to quantify the response of the Patagonian glaciers to climate change and their contribution to future sea-level rise. While the change in ice masses is a vivid example of the response to reduced precipitation, it also opens new perspectives for future studies on environmental change in Patagonia and can also help reduce uncertainties in the quantification of other precipitation-driven environmental phenomena.

Deleted: on the basis of

Deleted: ~30-50

Deleted: clearly

Deleted: Assuming that changes in the orographically induced precipitation is proportional to the moisture changes

Acknowledgments, Samples, and Data

This work was supported by the German Research Foundation (DFG), no. SA 2339/4-1. I would like to thank Manuel Gebetsberger, Emily Collier, Thomas Mölg, and Nicolas Cullen for the discussion and support. The simulations were

calculated on the High-Performance Cluster (HPC) at the Regional Computation Center (RRZE) of the University of Erlangen-Nürnberg.

Data and materials availability: Data were obtained from the European Centre for Medium-Range Forecast (ECMWF), the National Aeronautics and Space Administration (NASA), Consortium for Spatial Information (CGIAR-CSI), and Integrated Global Radiosonde Archive (IGRA) from the National Centers for Environmental Information (NCEI). SSM/I and SSMIS data are produced by Remote Sensing Systems. Data are available at www.remss.com/missions/ssmi.

References

Aracena, C., Lange, C. B., Iriarte, J. L., Rebolledo, L. and Pantoja, S.: Latitudinal patterns of export production recorded in surface sediments of the Chilean Patagonian fjords (41-55 S) as a response to water column productivity, Cont. Shelf Res., 31(3–4), 340–355, 2011.

Aravena, J. C. and Luckman, B. H.: Spatio-temporal rainfall patterns in Southern South America, Int. J. Climatol., 29, 2106–2120, doi:10.1002/joc, 2009.

Barrett, B. S., Garreaud, R. and Falvey, M.: Effect of the Andes Cordillera on Precipitation from a Midlatitude Cold Front, Mon. Weather Rev., 137(9), 3092–3109, doi:10.1175/2009MWR2881.1, 2009.

Bown, F., Rivera, A., Pętlicki, M., Bravo, C., Oberreuter, J. and Moffat, C.: Recent ice dynamics and mass balance of Jorge Montt Glacier, Southern Patagonia Icefield, J. Glaciol., 65(253), 732–744, doi:10.1017/jog.2019.47, 2019.

Bravo, C., Bozkurt, D., Gonzalez-Reyes, Á., Quincey, D. J., Ross, A. N., Farías-Barahona, D. and Rojas, M.: Assessing Snow Accumulation Patterns and Changes on the Patagonian Icefields, Front. Environ. Sci., 7, 30, doi:10.3389/fenvs.2019.00030, 2019.

Dee, D. P., Uppala, S. M., Simmons, A. J., Berrisford, P., Poli, P., Kobayashi, S., Andrae, U., Balmaseda, M. A., Balsamo, G., Bauer, P., Bechtold, P., Beljaars, A. C. M., van de Berg, L., Bidlot, J., Bormann, N., Delsol, C., Dragani, R., Fuentes, M., Geer, A. J., Haimberger, L., Healy, S. B., Hersbach, H., Hólm, E. V., Isaksen, L., Kållberg, P., Köhler, M., Matricardi, M., McNally, A. P., Monge-Sanz, B. M., Morcrette, J.-J., Park, B.-K., Peubey, C., de Rosnay, P., Tavolato, C., Thépaut, J.-N. and Vitart, F.: The ERA-Interim reanalysis: configuration and performance of the data assimilation system, Q. J. R. Meteorol. Soc., 137(656), 553–597, doi:10.1002/qj.828, 2011a.

Dee, D. P., Uppala, S. M., Simmons, A. J., Berrisford, P., Poli, P., Kobayashi, S., Andrae, U., Balmaseda, M. A., Balsamo, G., Bauer, P., Bechtold, P., Beljaars, A. C. M., van de Berg, L., Bidlot, J., Bormann, N., Delsol, C., Dragani, R., Fuentes, M., Geer, A. J., Haimberger, L., Healy, S. B., Hersbach, H., Hólm, E. V., Isaksen, L., Kållberg, P., Köhler, M., Matricardi, M., Mcnally, A. P., Monge-Sanz, B. M., Morcrette, J. J., Park, B. K., Peubey, C., de Rosnay, P., Tavolato, C., Thépaut, J. N. and Vitart, F.: The ERA-Interim reanalysis: Configuration and performance of the data assimilation system, Q. J. R. Meteorol. Soc., 137(656), 553–597, doi:10.1002/qj.828, 2011b.

Durre, I., Vose, R. S. and Wuertz, D. B.: Overview of the integrated global radiosonde archive, J. Clim., 19(1), 53–68, doi:10.1175/JCLI3594.1, 2006.

Escobar, F.: Water balance in the Patagonia Icefield, Glaciol. Res. Patagon. 1990, 109–119, 1992.

Falvey, M. and Garreaud, R.: Wintertime Precipitation Episodes in Central Chile: Associated Meteorological Conditions and Orographic Influences, J. Hydrometeorol., 8(2), 171–193, doi:10.1175/JHM562.1, 2007.

Foresta, L., Gourmelen, N., Weissgerber, F., Nienow, P., Williams, J. J., Shepherd, A., Drinkwater, M. R. and Plummer, S.: Heterogeneous and rapid ice loss over the Patagonian Ice Fields revealed by CryoSat-2 swath radar altimetry, Remote Sens. Environ., 211, 441–455, 2018.

Garreaud, R., Falvey, M., Montecinos, A., Garreaud, R., Falvey, M. and Montecinos, A.: Orographic Precipitation in Coastal Southern Chile: Mean Distribution, Temporal Variability, and Linear Contribution, J. Hydrometeorol., 17(4), 1185–1202, doi:10.1175/JHM-D-15-0170.1, 2016.

Garreaud, R. D.: Precipitation and circulation covariability in the extratropics, J. Clim., 20(18), 4789–4797, doi:10.1175/JCLI4257.1, 2007.

Garreaud, R. D.: The Andes climate and weather, Adv. Geosci., 22, 3–11, doi:10.5194/adgeo-22-3-2009, 2009.

Garreaud, R. D. and Muñoz, R. C.: The Low-Level Jet off the West Coast of Subtropical South America: Structure and Variability, Mon. Weather Rev., 133(12), 2246–2261, doi:10.1175/MWR3074.1, 2005.

Garreaud, R. D., Lopez, P., Minvielle, M. and Rojas, M.: Large-scale control on the Patagonian climate, J. Clim., 26(1), 215–230, doi:10.1175/JCLI-D-12-00001.1, 2013.

Held, I. M., Soden, B. J., Held, I. M. and Soden, B. J.: Robust Responses of the Hydrological Cycle to Global Warming, J. Clim., 19(21), 5686–5699, doi:10.1175/JCLI3990.1, 2006.

Jarosch, A. H., Anslow, F. S. and Clarke, G. K. C.: High-resolution precipitation and temperature downscaling for glacier models, Clim. Dyn., 38(1–2), 391–409, doi:10.1007/s00382-010-0949-1, 2012.

Jarvis, A., Reuter, H. I., Nelson, A. and Guevara, E.: Hole-filled SRTM for the globe Version 4, 2008.

Jobbágy, E. G., Sala, O. E. and Paruelo, J. M.: Patterns and controls of primary production in the Patagonian steppe: a remote sensing approach, Ecology, 83(2), 307–319, 2002.

Killick, R., Fearnhead, P. and Eckley, I. A.: Optimal detection of changepoints with a linear computational cost, J. Am. Stat. Assoc., 107(500), 1590–1598, doi:10.1080/01621459.2012.737745, 2012.

Landaeta, M. F., López, G., Suárez-Donoso, N., Bustos, C. A., Balbontiín, F. and Balbontín, F.: Larval fish distribution, growth and feeding in Patagonian fjords: potential effects of freshwater discharge, Environ. Biol. Fishes, 93(1), 73–87, doi:10.1007/s10641-011-9891-2, 2012.

Langhamer, L., Sauter, T. and Mayr, G. J.: Lagrangian Detection of Moisture Sources for the Southern Patagonia Icefield (1979–2017), Front. Earth Sci., 6, doi:10.3389/feart.2018.00219, 2018a.

Langhamer, L., Sauter, T. and Mayr, G. J.: Lagrangian Detection of Moisture Sources for the Southern Patagonia Icefield (1979–2017), Front. Earth Sci., 6, 219, doi:10.3389/feart.2018.00219, 2018b.

Lenaerts, J. T. M., Van Den Broeke, M. R., van Wessem, J. M., van de Berg, W. J., van Meijgaard, E., van Ulft, L. H., Schaefer, M. and Bilt, D.: Extreme precipitation and climate gradients in Patagonia revealed by high-resolution regional atmospheric climate modeling, J. Clim., 27(12), 4607–4621, doi:10.1175/JCLI-D-13-00579.1, 2014.

Malz, P., Meier, W., Casassa, G., Jaña, R., Skvarca, P. and Braun, M. H.: Elevation and mass changes of the Southern Patagonia Icefield derived from TanDEM-X and SRTM Data, Remote Sens., 10(2), 188, 2018.

Marshall, G. J., Thompson, D. W. J. and van den Broeke, M. R.: The Signature of Southern Hemisphere Atmospheric Circulation Patterns in Antarctic Precipitation, Geophys. Res. Lett., 44(22), 11,580-11,589, doi:10.1002/2017GL075998, 2017.

Marzeion, B., Jarosch, A. H. and Hofer, M.: Past and future sea-level change from the surface mass balance of glaciers, Cryosph., 6(6), 1295–1322, 2012.

Massmann, A. K., Minder, J. R., Garreaud, R. D., Kingsmill, D. E., Valenzuela, R. A., Montecinos, A., Fults, S. L. and Snider, J. R.: The Chilean Coastal Orographic Precipitation Experiment: Observing the Influence of Microphysical Rain Regimes on Coastal Orographic Precipitation, J. Hydrometeorol., 18(10), 2723–2743, doi:10.1175/jhm-d-17-0005.1, 2017.

Mayr, C., Langhamer, L., Wissel, H., Meier, W., Sauter, T., Laprida, C., Massaferro, J., Försterra, G. and Lücke, A.: Atmospheric controls on hydrogen and oxygen isotope composition of meteoric and surface waters in Patagonia, Hydrol. Earth Syst. Sci. Discuss., 1–22, doi:10.5194/hess-2018-431, 2018.

Mernild, S. H., Liston, G. E., Hiemstra, C. and Wilson, R.: The Andes Cordillera. Part III: glacier surface mass balance and contribution to sea level rise (1979–2014), Int. J. Climatol., 37(7), 3154–3174, doi:10.1002/joc.4907, 2017.

Muñoz, R. C. and Garreaud, R. D.: Dynamics of the Low-Level Jet off the West Coast of Subtropical South America, Mon. Weather Rev., 133(12), 3661–3677, 2005.

Press, W. H., Teukolsky, S. A., Vetterling, W. T. and Flannery, B. P.: Numerical recipes 3rd edition: The art of scientific computing, Cambridge university press., 2007.

Rasmussen, L. A., Conway, H. and Raymond, C. F.: Influence of upper air conditions on the Patagonia icefields, , 59, 203–216, doi:10.1016/j.gloplacha.2006.11.025, 2007.

Rignot, E., Rivera, A. and Casassa, G.: Contribution of the Patagonia Icefields of South America to Sea Level Rise, Science (80-.)., 302(5644), 434–437, doi:10.1126/science.1087393, 2003.

Schaefer, M., Machguth, H., Falvey, M. and Casassa, G.: Modeling past and future surface mass balance of the Northern Patagonia Icefield, J. Geophys. Res. Earth Surf., 118(2), 571–588, doi:10.1002/jgrf.20038, 2013.

Schaefer, M., MacHguth, H., Falvey, M., Casassa, G. and Rignot, E.: Quantifying mass balance processes on the Southern Patagonia Icefield, Cryosphere, 9(1), 25–35, doi:10.5194/tc-9-25-2015, 2015.

Schneider, C. and Gies, D.: Effects of El Niño-southern oscillation on southernmost South America precipitation at 53°S revealed from NCEP-NCAR reanalyses and weather station data, Int. J. Climatol., 24(9), 1057–1076, doi:10.1002/joc.1057, 2004.

Schneider, C., Glaser, M., Kilian, R., Santana, A., Butorovic, N. and Casassa, G.: Weather Observations Across the Southern

Andes at 53°S, Phys. Geogr., 24(2), 97–119, doi:10.2747/0272-3646.24.2.97, 2003.

Schneider, T., O'Gorman, P. a., Levine, X. J., Gorman, P. A. O. and Levine, X. J.: Water vapor and the dynamics of climate changes, Rev. Geophys., (48), 1–22, doi:10.1029/2009RG000302.1.INTRODUCTION, 2010.

Schwikowski, M., Brütsch, S., Casassa, G. and Rivera, A.: A potential high-elevation ice-core site at Hielo Patagónico Sur, Ann. Glaciol., 43, 8–13, 2006.

Shiraiwa, T., Kohshima, S., Uemura, R., Yoshida, N., Matoba, S., Uetake, J. and Godoi, M. A.: High net accumulation rates at Campo de Hielo Patagonico Sur, South America, revealed by analysis of a 45.97 m long ice core, Ann. Glaciol., 35(1), 84–90, 2002.

Smith, R. B. and Barstad, I.: A Linear Theory of Orographic Precipitation, J. Atmos. Sci., 61(12), 1377–1391, 2004.

Smith, R. B. and Evans, J. P.: Orographic Precipitation and Water Vapor Fractionation over the Southern Andes, J. Hydrometeorol., 8(1), 3–19, doi:10.1175/JHM555.1, 2007.

Thompson, D. W. J. and Solomon, S.: Interpretation of recent Southern Hemisphere climate change, Science (80-.)., 296(5569), 895–899, doi:10.1126/science.1069270, 2002.

Trenberth, K. E., Fasullo, J. and Smith, L.: Trends and variability in column-integrated atmospheric water vapor, Clim. Dyn., 24(7–8), 741–758, doi:10.1007/s00382-005-0017-4, 2005.

Vallis, G. K., Zurita-gotor, P., Cairns, C. and Kidston, J.: Response of the Large-Scale Structure of the Atmosphere to Global Warming, Q. J. R. Meteorol. Soc., 141(0000), 1–27, doi:10.1002/qj.2456, 2014.

Vargas, C. A., Cuevas, L. A., Silva, N., González, H. E., Pol-Holz, D., Narváez, D. A. and others: Influence of Glacier Melting and River Discharges on the Nutrient Distribution and DIC Recycling in the Southern Chilean Patagonia, J. Geophys. Res. Biogeosciences, 123(1), 256–270, 2018.

Viale, M. and Garreaud, R.: Orographic effects of the subtropical and extratropical Andes on upwind precipitating clouds, J. Geophys. Res. Atmos., 120(10), 4962–4974, 2015.

Viale, M., Houze, R. A., Rasmussen, K. L., Viale, M., Jr., R. A. H. and Rasmussen, K. L.: Upstream Orographic Enhancement of a Narrow Cold-Frontal Rainband Approaching the Andes, Mon. Weather Rev., 141(5), 1708–1730, doi:10.1175/MWR-D-12-00138.1, 2013.

Waliser, D. and Guan, B.: Extreme winds and precipitation during landfall of atmospheric rivers, Nat. Geosci., 10(3), 179–183, doi:10.1038/ngeo2894, 2017.

Weidemann, S., Sauter, T., Schneider, L. and Schneider, C.: Impact of two conceptual precipitation downscaling schemes on mass-balance modeling of Gran Campo Nevado ice cap, Patagonia, J. Glaciol., 59(218), 1106–1116, doi:10.3189/2013JoG13J046, 2013.

Weidemann, S., Sauter, T., Malz, P., Jaña, R., Arigony-Neto, J., Casassa, G. and Schneider, C.: Glacier Mass Changes of Lake-Terminating Grey and Tyndall Glaciers at the Southern Patagonia Icefield Derived From Geodetic Observations and Energy and Mass Balance Modeling, Front. Earth Sci., 6, 81, doi:10.3389/feart.2018.00081, 2018a.

Weidemann, S. S., Sauter, T., Kilian, R., Steger, D., Butorovic, N. and Schneider, C.: A 17-year Record of Meteorological

Observations Across the Gran Campo Nevado Ice Cap in Southern Patagonia, Chile, Related to Synoptic Weather Types and Climate Modes, Front. Earth Sci., 6, doi:10.3389/feart.2018.00053, 2018b.

Wentz, F. J., Spencer, R. W., Systems, R. S., Rosa, S. and Hydrology, G.: SSM/I rain retrievals within a unified all-weather ocean algorithm, J. Atmos. Sci., 55(9), 1613–1627, 1998.

Willis, M. J., Melkonian, A. K., Pritchard, M. E. and Rivera, A.: Ice loss from the Southern Patagonian ice field, South America, between 2000 and 2012, Geophys. Res. Lett., 39(17), 2012.

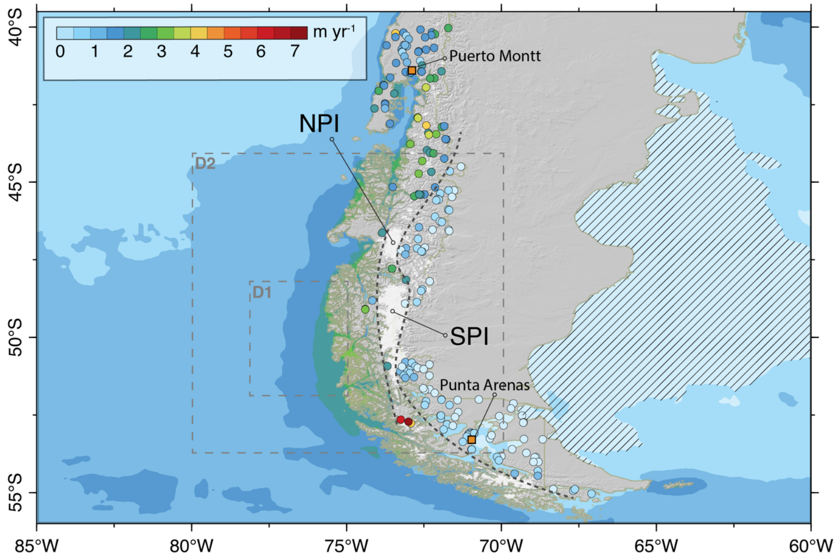

Figure 1: Precipitation climatology in southern South America. The filled circles indicate precipitation amounts measured by the observational network, established by the Dirección Meteorológica de Chile (DMC), Dirección General de Aguas (DGA), and own weather stations (see Table S1). The colour shaded areas over the ocean shows the rainfall distribution based on the Global Precipitation Measurement (GPM) satellite mission. Black dashed lines roughly delineate the maritime Pre-Cordillera range, Andes main ridge, and the semiarid Pampa region. Also indicated are the Northern (NPI) and Southern Patagonian Icefields (SPI). The dashed area shows the semi-arid rain-shadow region. Also shown are the simulation (D2) and forcing (D1) domains.

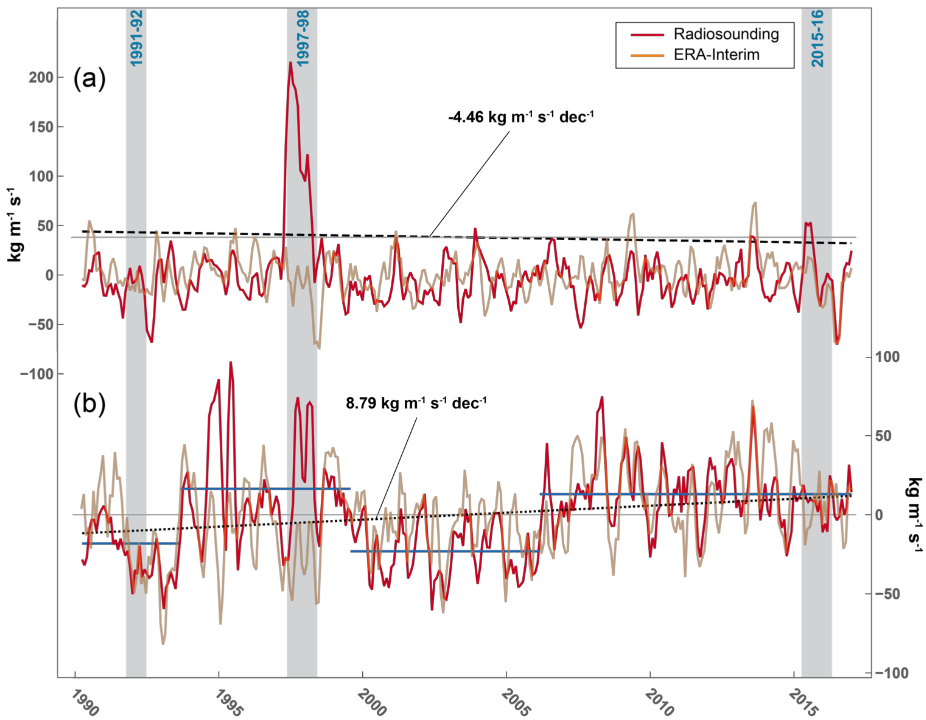

Figure 2: Monthly WVF anomalies in Puerto Montt (panel a) and Punta Arenas (panel b). Shown are the running 3-month mean WVF anomalies for the atmospheric soundings and the nearest ERA-Interim grid point from 1990-2016. The blue shaded areas indicate very strong El Niño events (ONI>1.5). The horizontal blue lines in panel b show the mean WVF over water vapor rich and poor phases.

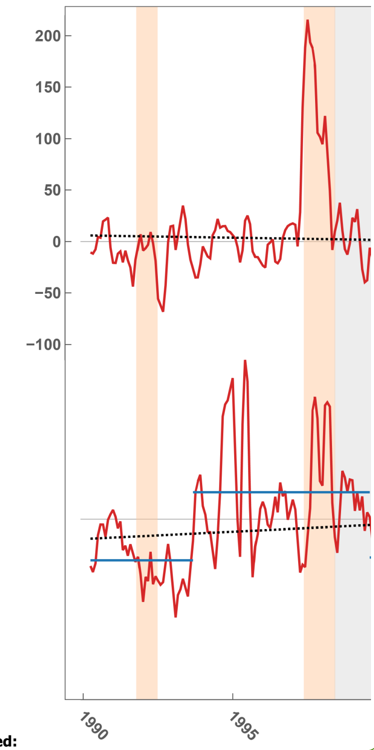

Deleted:

Deleted: Monthly WVF anomalies.

Deleted: Atmospheric soundings for (A) Puerto Montt and (B) Punta Arenas from 1990 to 2016.

Deleted: orange

Deleted: , while the grey shaded areas indicate strong La Niña events (ONI<-1.5)

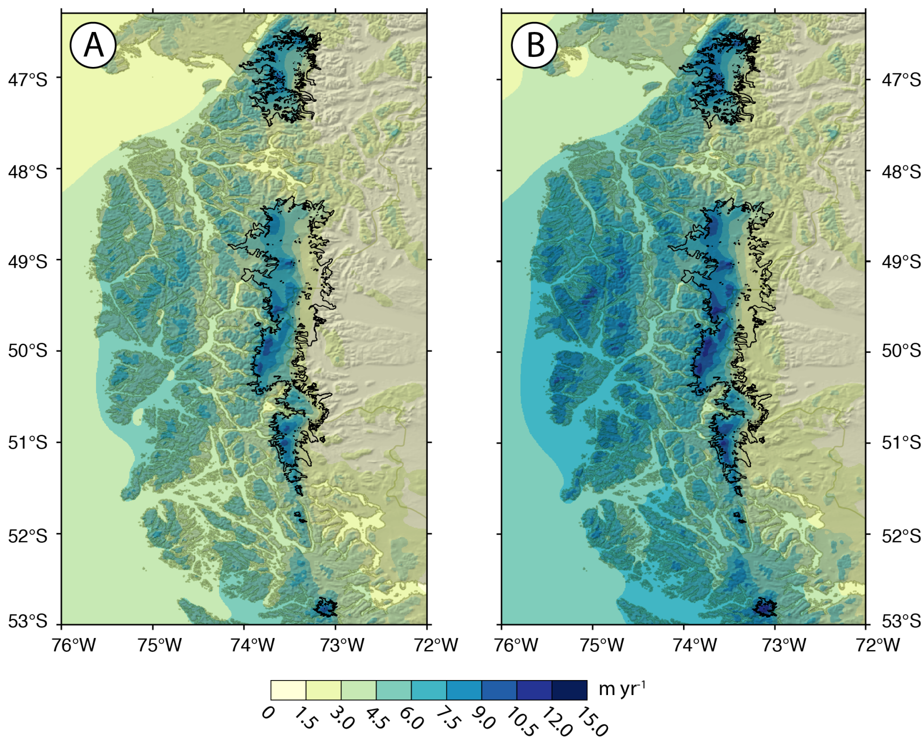

Figure 3: Results of the OPM ensemble experiments. Mean precipitation fields simulated by the OPM using (A) the 'realistic' (DR=0.45) parameter setup, and (B) the 'extreme' parameter setup using a DR of 0.6 and the 98th percentile values for the uplift sensitivity factor (C_w=0.004) and moist stability frequency (Nm=0.007).

Formatted: Subscript

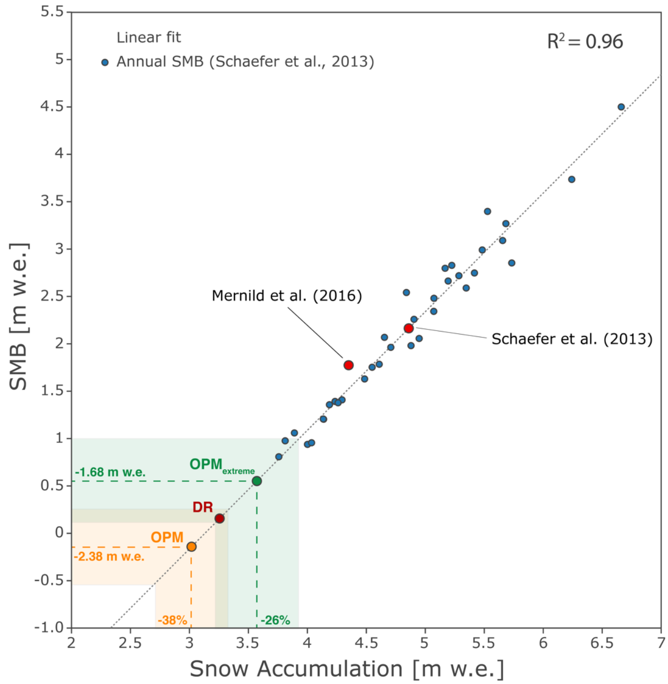

Figure 4: Relation between the annual specific accumulation and surface mass balance over the SPI from 1975-2000. The red and blue dots mark the multi-annual mean values using the accumulation rates from Schaefer et al. (2013) and Mernild et al. (2016), respectively. The values obtained by this study are represented by the green, orange and dark red dots. The shaded areas mark lower and upper snow accumulation and SMB bounds derived from the DR-scaling (DR), the realistic (OPM) and extreme (OPM$_{extreme}$) orographic precipitation model experiments. The percentage and numbers show the differences between the current study and the values given by Schaefer et al..

Deleted: , green

Deleted: and orange

Deleted: ,

Deleted: and

Deleted: , respectively

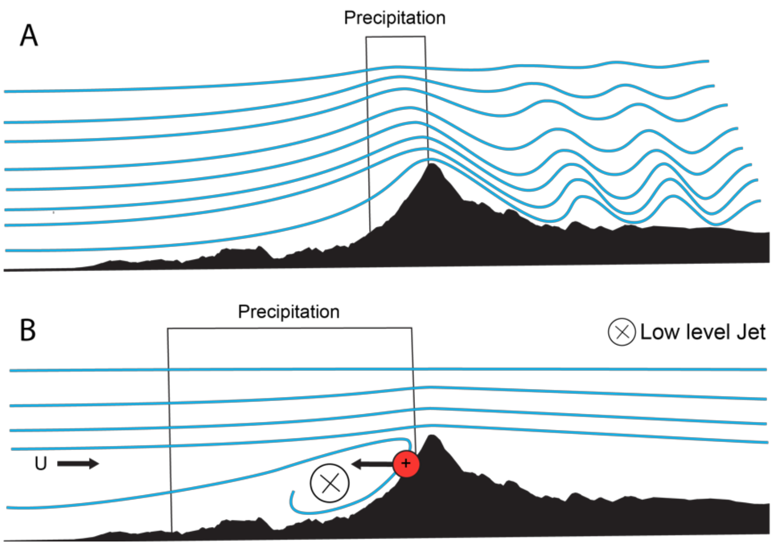

Figure 5: Schematic illustration of the interaction between the atmospheric air flow and the Andes. (A) Linear mountain flow response ($\hat{H}<1$) leads to strong uplift and precipitation along the west slopes. (B) The air flow is blocked by the topography ($H\geq1$) and the resulting pressure gradient (indicated by the red circle) at the west slope slows down the upstream flow. The imbalance between the large-scale pressure gradient and Coriolis-force leads to a northerly low-level jet, which reduces and shifts the uplift motions upstream. This mechanism enhances precipitation in the Pre-Cordillera range, while reducing precipitation at the west slopes of the Andes.

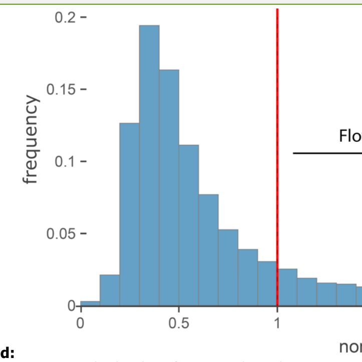

Deleted:
Figure 5: Frequency distribution of the non-dimensional mountain height. The non-dimensional mountain height is calculated from ERA-Interim data (2010-2016) off Patagonia's west coast (Fig. 1, D1).

Page Break

Deleted: 6

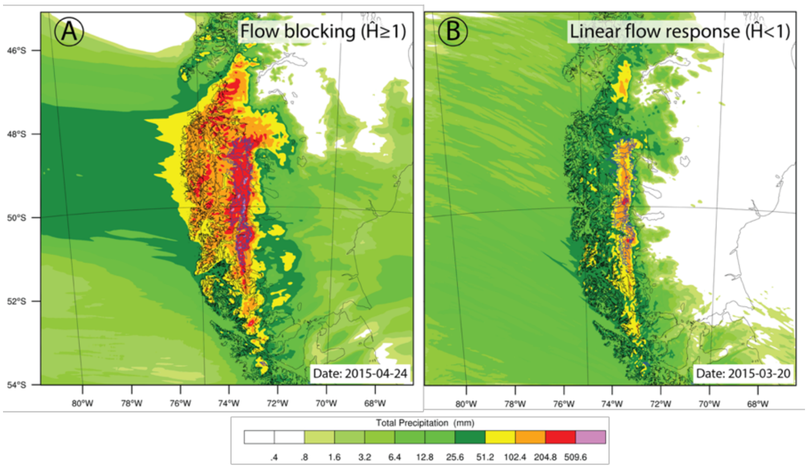

Figure 6: Total precipitation sums (3-days) over the SPI and NPI from WRF for different flow regimes. (A) Nonlinear flow response with enhanced precipitation in the Pre-Cordillera range and (B) linear flow response with strong localized precipitation along the west slopes of the Andes.

Deleted: 7

Table 1: Comparison of mean precipitation estimates on the SPI and NPI averaged over the entire Icefield and the western and eastern slopes. Values are given in m w.e. yr^{-1}. The local maximum values, if available, are shown in parentheses.

Formatted: Superscript

	SPI			NPI			Period
	Mean	West	East	Mean	West	East	
Realistic scenario (mean)	5.06±0.51 (10.09±0.92)	5.93±0.60 (10.09±0.92)	4.06±0.42 (9.92±0.95)	5.38±0.59 (9.43±0.93)	5.83±0.64 (9.43±0.93)	4.37±0.48 (9.30±0.92)	2010-2016
> 3000 m	8.03±0.81	8.60±0.85	8.10±0.82	7.16±0.79	7.40±0.78	6.66±0.73	
2500–3000 m	6.37±0.65	6.93±0.70	6.13±0.63	6.58±0.67	6.84±0.70	5.58±0.53	
2000-2500 m	5.39±0.54	5.70±0.58	4.93±0.50	5.69±0.58	6.20±0.63	5.10±0.52	
1000-2000 m	5.29±0.54	6.13±0.62	4.26±0.44	5.58±0.62	5.77±0.64	4.81±0.53	
< 1000 m	4.26±0.44	5.43±0.56	3.04±0.32	4.81±0.54	5.77±0.64	3.05±0.35	
Extreme scenario (mean)	5.99±0.59 (11.58±0.98)	7.02±0.68 (11.58±0.98)	4.80±0.49 (11.39±0.99)	6.09±0.64 (10.37±0.96)	6.60±0.69 (10.37±0.96)	4.90±0.53 (10.12±0.95)	2010-2016
> 3000 m	8.89±0.89	9.56±0.94	8.94±0.90	7.67±0.85	7.93±0.85	7.07±0.79	
2500–3000 m	7.09±0.73	7.73±0.78	6.81±0.71	7.05±0.73	7.35±0.75	5.92±0.59	
2000-2500 m	6.08±0.61	6.46±0.65	5.55±0.57	6.16±0.64	6.75±0.69	5.48±0.57	
1000-2000 m	6.19±0.61	7.17±0.70	5.00±0.52	6.21±0.67	6.45±0.70	5.30±0.58	
< 1000 m	5.34±0.53	6.77±0.66	3.84±0.39	5.74±0.58	6.84±0.68	3.72±0.40	
DR-scaling (mean)	5.46±1.30 (8.99±3.33)			5.38±1.26 (9.63±3.69)			2010-2016
Other studies							
Schaefer et al. (2015)	8.36 (>20.0)			8.03±0.37 (>15.0)			1975-2011
Mernild et al. (2016)	8.13±0.32 (>15.0)			6.95±0.34 (>15.0)			1979-2014
Lenaerts et al. (2013)	- (>30.0)			- (>30.0)			1979-2012
Escobar et al. (1992)	7.0			6.7 (over the broad plateau)			1960-1980

Formatted Table

Commented [A1]: New colums added

Deleted: 10

Revisiting extreme precipitation amounts over southern South America and implications for the Patagonian Icefields

Tobias Sauter[1]

[1]Climate System Research Group, Institute of Geography, Friedrich-Alexander-University Erlangen-Nürnberg (FAU), Germany

Correspondence to: Tobias Sauter (tobias.sauter@fau.de)

Contents of this file

Deleted: 3

Deleted: 3

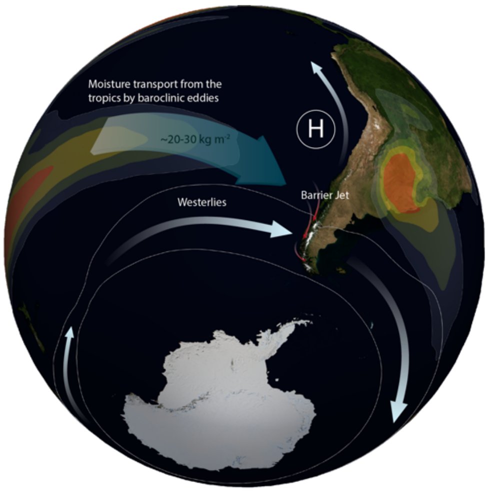

Figure S1: Schematic illustration of the atmospheric large-scale circulation and moisture transport in the South Pacific. Shown are the location of the westerlies for austral summer (December-January-February), the barrier jet along the Andes (red arrows), and the mean moisture transport by baroclinic eddies (blue shaded arrow). The shading indicates regions of high water vapor variability.

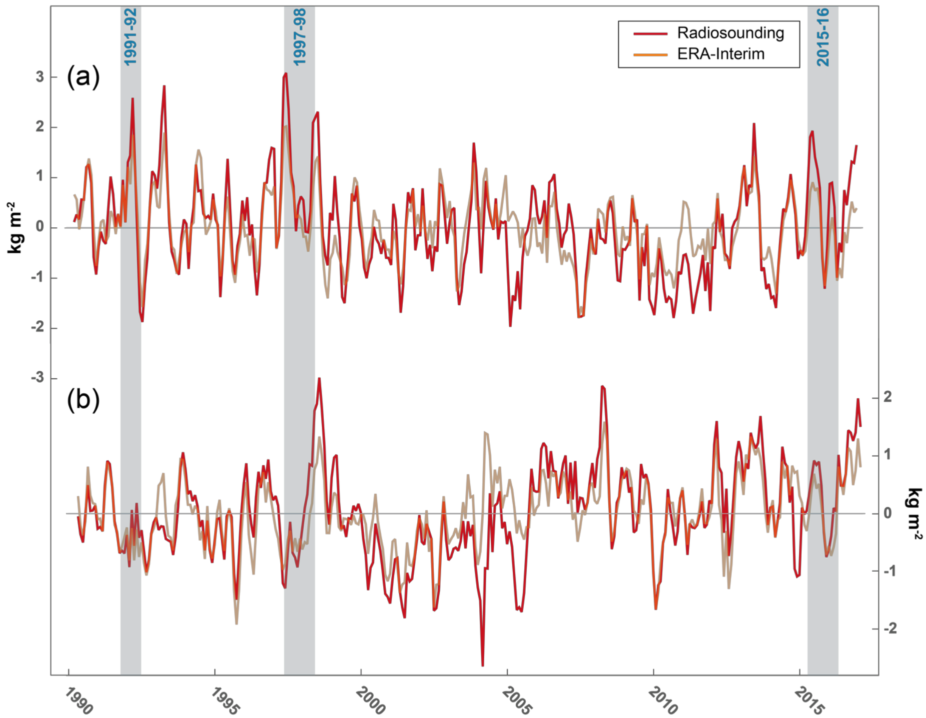

Figure S2: Monthly IWV anomalies in Puerto Montt (panel a) and Punta Arenas (panel b). Shown are the running 3-month mean IWV anomalies for the atmospheric soundings and the nearest ERA-Interim grid point from 1990-2016. The blue shaded areas indicate very strong El Niño events (ONI>1.5).

Deleted: 1

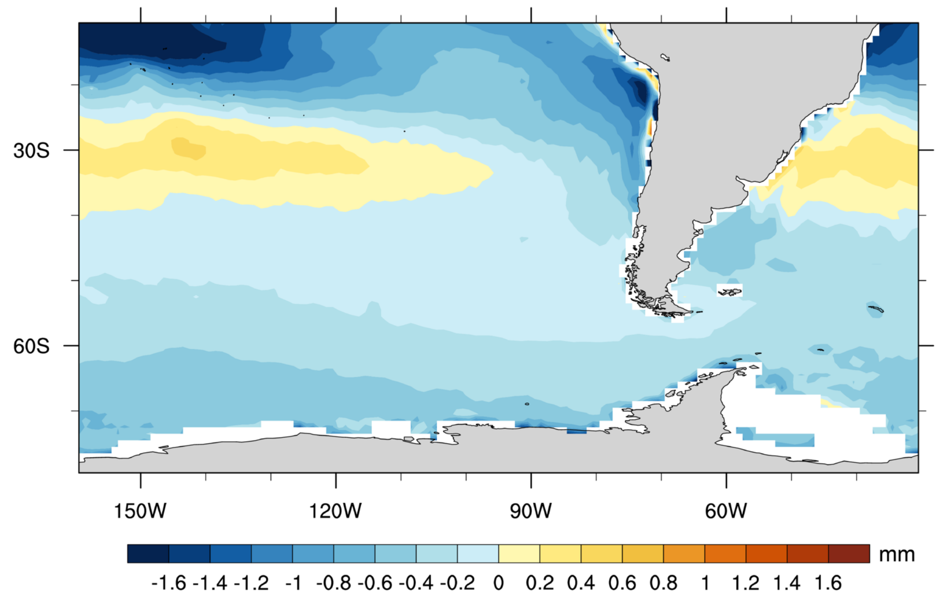

Figure S3: Mean differences in the IWV between ERA Interim and SSMI data for the period 1988-2016. Red shading indicates a positive bias in the ERA Interim data.

Deleted: 2

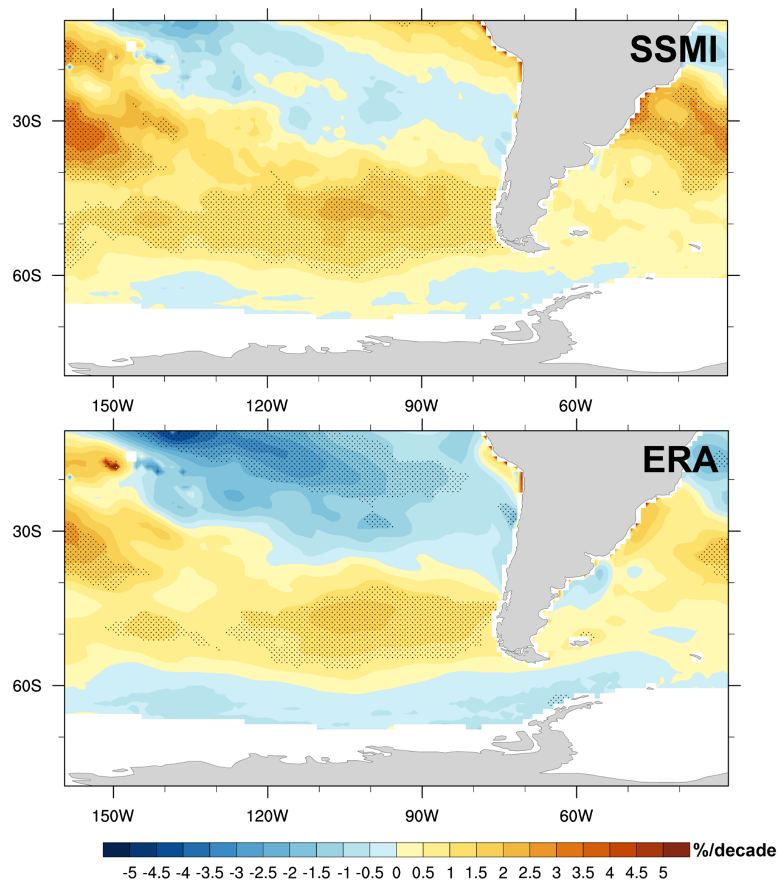

Figure S4: Linear trend of IWV in the SSM/I and ERA-Interim data for the period 1988-2016 (in % per decade). Dotted areas indicate significant long-term trends (p<0.05).

Deleted: 3

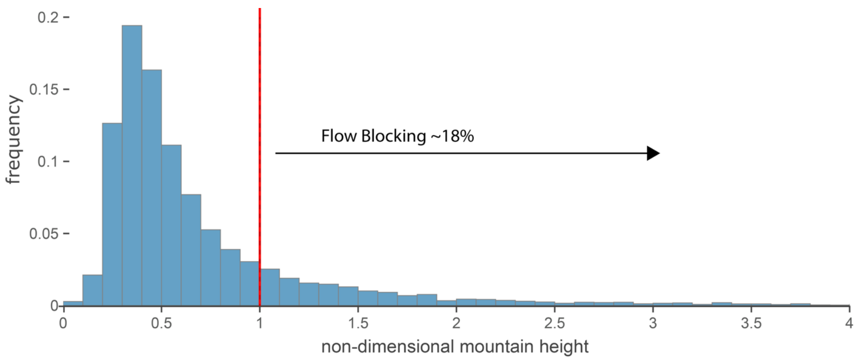

5 **Figure S5: Frequency distribution of the non-dimensional mountain height. The non-dimensional mountain height is calculated from ERA-Interim data (2010-2016) off Patagonia's west coast (Fig. 1, D1).**

Table S1.Automatic weather stations in Patagonia. Precipitation sums and trends are given in mm. Bold numbers indicate significant trends (p<0.05).

Station	**Lat**	**Lon**	**Sum**	**Trend in % per decade**	**from**	**to**
Pirihueico En Pirihueico	-40.02	-71.72	2875	**-0.36**	1999	2015
El Llolly	-40.07	-72.62	1763	-0.02	1995	2015
Catamutun	-40.17	-73.17	1858	0.02	1998	2015
Venecia	-40.19	-73.43	3964	-0.04	1998	2015
Lago Maihue	-40.22	-72.15	2982	**-0.17**	1980	2015
Trinidad	-40.31	-73.43	1713	0.13	1998	2015
Lago Ranco	-40.32	-72.47	1923	0.01	1980	2015
Adolfo Matthei	-40.59	-73.11	1256	-0.05	1983	2016
Canal Bajo Osorno Ad.	-40.61	-73.06	1232	-0.04	1980	2016
Anticura	-40.66	-72.18	1185	-0.39	1998	2015
Rio Negro En Chahuilco	-40.71	-73.23	1240	-0.21	2004	2016
Futacuhuin	-40.72	-72.44	1681	-0.07	1995	2015
Rupanco	-40.77	-72.68	1665	-0.04	1994	2015
San Antonio Oeste Aero	-40.78	-65.10	202	**0.25**	1980	2016
Gobernador Castello	-40.87	-63.00	272	**0.21**	1980	2016
Purranque	-40.94	-73.14	1309	0.00	1999	2015
Frutillar	-41.13	-73.06	1467	0.00	1994	2015
San Carlos De Bariloche	-41.15	-71.16	589	**0.21**	1980	2016
Fresia	-41.15	-73.41	1613	-0.03	1994	2015
La Ensenada	-41.23	-72.57	2358	0.00	1980	2005
Maquinchao	-41.25	-68.73	96	0.25	1980	2016
Lago Chapo	-41.42	-72.60	3038	-0.05	1999	2014
El Tepual Puerto Montt Ap.	-41.44	-73.10	1590	-0.05	1980	2016
Puerto Montt	-41.46	-72.94	1845	0.00	1980	2016
Puerto Montt	-41.46	-72.94	1845	0.00	1980	2016
Maullin	-41.62	-73.60	1668	-0.04	1987	2015
Puelo	-41.65	-72.31	2642	-0.17	1997	2016
Ancud 1 (Dga)	-41.86	-73.82	2013	0.12	1993	2015
Hornopiren	-41.94	-72.44	2971	**-0.49**	1998	2016
El Bolson	-41.94	-71.53	232	**1.02**	1996	2016

Formatted: Caption

Chepu	-42.05	-73.97	2554	-0.08	1999	2015
Quemchi	-42.14	-73.47	2437	-0.03	2000	2015
Castro 1 (Dga)	-42.46	-73.77	1555	**-0.37**	1993	2008
Cucao	-42.62	-74.11	2067	0.05	1997	2015
Chaiten	-42.91	-72.71	3408	0.26	1998	2007
Chaiten Ad.	-42.93	-72.70	3590	-0.02	1980	2007
Esquel Aero	-42.93	-71.15	372	**0.18**	1980	2016
Quellon	-43.11	-73.61	1781	0.01	1993	2015
Puerto. Cardenas	-43.18	-72.43	3922	-0.33	2001	2015
Futaleufu Ad.	-43.19	-71.85	1958	-0.01	1980	2016
Trelew Aero	-43.20	-65.27	171	0.11	1980	2016
Lago Espolon	-43.22	-71.93	2693	-0.13	2001	2015
Valle Rio Frio	-43.47	-72.35	3712	**-0.24**	2001	2015
Christchurch Intl	-43.49	172.53	486	**0.05**	1980	2016
Cape Bruny Lighthouse	-43.49	147.15	940	-0.07	1980	2016
Alto Palenaad.	-43.61	-71.81	1589	-0.04	1980	2016
Palena	-43.62	-71.78	1597	**-0.20**	2001	2015
Maatsuyker Island Lighthouse	-43.66	146.27	1235	**-0.16**	1980	2016
Marin Balmaceda	-43.77	-72.95	2388	0.17	1994	2015
Paso De Indios	-43.82	-68.88	86	0.44	1980	1996
Chatham Islands Aws	-43.95	-176.57	624	0.16	1994	2011
La Junta	-43.97	-72.41	1998	-0.07	1981	2016
Bordalit	-44.05	-72.32	2508	**-0.29**	1994	2011
Lago Verde	-44.24	-71.85	1244	0.41	1994	2011
Puerto Puyuhuapi	-44.32	-72.56	2994	-0.08	1981	2015
Rio Cisnes	-44.50	-71.31	273	**-0.26**	1981	2015
La Tapera	-44.65	-71.67	687	-0.29	1981	2002
Cisnes Medio	-44.67	-72.27	2162	0.00	1982	2015
Puerto Cisnes	-44.73	-72.68	2812	-0.09	1981	2015
Villa Maihuales	-45.17	-72.15	1399	-0.09	1986	2015
Estancia Bao Nuevo	-45.27	-71.53	490	-0.01	2001	2015
Irehuao	-45.27	-71.71	409	0.11	1994	2015
Villa Ortega	-45.37	-71.98	654	-0.14	1981	2015
Puerto Aysen Ad.	-45.40	-72.66	2011	-0.11	1980	2016
Puerto Aysen	-45.40	-72.70	2197	**-0.32**	1994	2008
El Balseo	-45.40	-72.49	1745	-0.06	1981	2015

Rio Aysen En Puerto Aysen	-45.41	-72.62	1944	0.00	2003	2016
Puerto Chacabuco	-45.46	-72.82	2678	-0.05	1985	2015
Coyhaique Alto	-45.48	-71.60	221	0.02	1985	2016
Coyhaique Conaf	-45.55	-72.06	887	-0.19	2003	2015
Rio Simpson Bajo Junta Coyhaique	-45.55	-72.07	723	-0.24	2006	2016
Coyhaique (Escuela Agricola)	-45.57	-72.03	808	-0.06	1984	2016
Teniente Vidal Coyhaique Ad.	-45.59	-72.11	986	0.03	1980	2016
Comodoro Rivadavia	-45.78	-67.50	203	0.00	1980	2016
Balmaceda Ad.	-45.91	-71.69	529	-0.03	1980	2016
Villa Cerro Castillo	-46.12	-72.15	540	**-0.41**	1993	2015
Rio Ibaez En Desembocadura	-46.27	-71.99	490	0.26	2006	2016
Puerto Ibaez	-46.29	-71.93	396	**0.47**	1986	2008
Invercargill Airpor	-46.42	168.33	888	0.01	1980	2016
Alfred Faure (Iles Crozet)	-46.43	51.85	1652	0.02	1980	2016
Bahia Murta	-46.46	-72.67	1208	**-0.21**	1994	2015
Perito Moreno Arpt	-46.52	-71.02	74	-0.08	1980	2016
Chile Chico	-46.54	-71.71	228	-0.13	1994	2015
Chile Chico Ad.	-46.58	-71.69	255	-0.01	1980	2016
Puerto Guadal	-46.84	-72.70	565	0.31	1994	2015
Marion Island	-46.88	37.87	1857	**-0.12**	1980	2016
Estancia Valle Chacabuco	-47.12	-72.48	189	-0.29	1994	2015
Rio Baker En Angostura Chacabuco	-47.14	-72.73	745	0.05	2004	2016
Lord Cochrane Ad.	-47.24	-72.59	702	-0.07	1980	2016
Rio Cochrane En Cochrane	-47.25	-72.56	480	0.19	2005	2016
Puerto Deseado	-47.74	-65.90	66	-0.25	1980	2012
Caleta Tortel	-47.80	-73.54	1987	-0.13	2003	2016
Rio Pascua Ante Junta Rio Quetru	-48.16	-73.09	2082	-0.07	2004	2016
Rio Mayer Reten	-48.21	-72.32	200	1.07	1994	2003
Villa Ohiggins	-48.47	-72.56	771	**0.36**	1994	2008
Lago Ohiggins En Villa Ohiggins	-48.52	-72.60	895	-0.08	2004	2016
Gobernador Gregores	-48.78	-70.17	63	-0.85	1980	1996
Candelario Mancilla	-48.88	-72.74	458	0.05	1994	2016
Puerto Eden	-49.12	-74.41	2346	**-0.43**	1998	2010
San Julian	-49.31	-67.80	190	0.09	1980	2016
Port-Aux-Francais (Iles Kergu	-49.35	70.25	591	0.02	1980	2016
El Calafate Aero	-50.27	-72.05	145	-0.16	2004	2016

Lago Argentino Arpt	-50.33	-72.30	120	**0.98**	1980	1999
Enderby Island Aws	-50.48	166.30	737	0.07	1993	2016
Lago Dickson	-50.82	-73.11	910	**0.93**	2004	2016
Cerro Guido	-50.90	-72.33	265	**0.10**	1984	2016
Rio Las Chinas En Cerro Guido	-51.05	-72.52	226	0.29	2005	2016
Torres Del Paine	-51.18	-72.97	739	0.04	1983	2016
Cerro Castillo	-51.26	-72.33	315	0.00	1981	2016
Rio Gallegos Aero	-51.62	-69.28	214	**0.19**	1980	2016
Teniente Gallardo Puerto Natales Ad.	-51.67	-72.53	192	**1.69**	1999	2016
Casas Viejas	-51.70	-72.33	256	**0.24**	1981	2015
Puerto Natales	-51.73	-72.48	490	-0.02	1986	2016
Mount Pleasant	-51.82	-58.45	471	0.03	1992	2016
Rio Rubens En Ruta N 9	-52.03	-71.94	414	**-1.29**	2007	2016
Teniente Merino	-52.03	-70.73	221	0.09	1984	2015
Rubens En Ruta N. 9	-52.04	-71.94	473	**-0.52**	1990	2005
Rio Penitente En Morro Chico	-52.05	-71.42	265	-0.15	2007	2016
Monte Aymond	-52.16	-69.61	250	-0.03	1996	2016
Villa Tehuelche	-52.44	-71.40	337	-0.04	1981	2016
Rio Perez	-52.55	-71.96	525	-0.04	1990	2014
Campbell Island Aws	-52.55	169.17	1017	**0.44**	1996	2016
Seno Skyring	-52.55	-71.96	584	-0.56	2002	2016
San Gregorio	-52.57	-70.07	264	-0.03	1992	2016
Rio Verde	-52.60	-71.50	337	0.02	1994	2016
Rocallosas	-52.65	-71.96	327	**-0.88**	1994	2015
Cerro Sombrero	-52.78	-69.29	248	-0.06	1984	2014
Bahamondes	-52.80	-72.93	3367	**-0.75**	2000	2015
Bahia San Felipe	-52.87	-69.93	351	0.12	1980	2016
Isla Riesco	-52.88	-71.57	408	-0.09	1991	2015
Punta Arenas	-53.12	-70.88	923	0.02	1980	2016
Canal De Trasvase Estero Llau-Llau	-53.13	-70.94	648	-0.10	2005	2016
Rio Las Minas En Bt. Sendos	-53.14	-70.99	780	-0.03	2000	2016
Las Minas	-53.14	-70.98	774	-0.14	1996	2015
Laguna Lynch	-53.14	-70.98	435	-0.04	1980	2015
Fuentes Martinez Porvenir Ad.	-53.19	-70.32	260	-0.03	1986	2016
Porvenir	-53.29	-70.37	315	**-0.20**	1991	2015
Onaisin En Maria Cristina	-53.31	-69.27	315	-0.12	1990	2016

San Sebastian	-53.32	-68.66	294	0.13	1990	2016
Lago Parrillar	-53.40	-71.25	800	0.00	1990	2016
Cameron	-53.64	-69.65	366	0.08	1994	2016
San Juan	-53.65	-70.96	544	**0.29**	1980	2016
Russfin	-53.76	-69.19	429	-0.01	1994	2016
Rio Caleta En Tierra Del Fuego	-53.86	-70.00	340	-0.15	2007	2016
Rio Grande En Tierra Del Fuego	-53.89	-68.88	276	0.14	2007	2016
Seccion Rio Grande	-53.90	-68.92	401	0.15	1991	2011
Pampa Huanaco	-54.05	-68.80	340	**0.28**	1994	2016
Macquarie Island	-54.50	158.94	912	-0.03	1980	2016
Ushuaia Malvinas Argentinas	-54.84	-68.30	335	0.24	1980	2016
Guardia Marina Zanartu Pto Williams	-54.93	-67.62	466	-0.09	1980	2016
Rio Robalo En Puerto Williams	-54.95	-67.64	389	0.14	2005	2016

Table S2. Comparison of the IWV trends between atmospheric soundings and the nearest ERA-Interim grid point. Numbers are given in mm decade^{-1}. Bold numbers indicate significant trends ($p<0.05$).

Deleted: 1

	1988-2016	1988-2009	2010-2016
Puerto Montt			
Radiosounding	-0.22 (-1.5%)	-0.42 (-3.0%)	2.87 (19.4%)
ERA-Interim	-0.16 (-1.3%)	-0.25 (-2.0%)	0.65 (5.2%)
Punta Arenas			
Radiosounding	0.23 (2.2%)	0.07 (0.6%)	1.23 (11.3%)
ERA-Interim	0.14 (1.3%)	0.05 (0.4%)	0.80 (7.0%)

Table S3. Comparison of the OPM (DR=0.45) with observations. Given are the latitude (lat), longitude (lon), altitude (alt), the precipitation values from the orographic precipitation model (OPM) and the observations (Obs) at the weather stations The precipitation values are given in mm yr^{-1}.

Deleted: 2

Location	lat	lon	alt	OPM	Obs
Villa Cerro Castillo	-46.12	-72.15	345	471.30	282.45
Rio Ibaez En Desembocadura	-46.26	-71.99	220	298.12	623.58
Bahia Murta	-46.46	-72.66	240	849.30	1017.93

Lago General Carrera Fachinal	-46.54	-72.22	18	579.54	333.60
Glaciar San Rafael	-46.64	-73.85	8	3829.02	1271.60
Puerto Guadal	-46.84	-72.70	210	745.45	656.28
Estancia Valle Chacabuco	-47.11	-72.48	343	613.92	159.60
Rio Nef Antes Junta Estero El Revalse	-47.13	-73.08	281	895.86	974.88
Rio Baker En Angostura Chacabuco	-47.14	-72.72	160	673.35	856.73
Lago Cachet 2 En Glaciar Colonia	-47.19	-73.25	427	1088.06	243.25
Lord Cochrane Ad.	-47.24	-72.58	204	744.24	652.65
Rio Cochrane En Cochrane	-47.25	-72.56	140	788.03	514.75
Rio Colonia En Nacimiento	-47.33	-73.11	146	986.30	1261.80
Caleta Tortel	-47.79	-73.53	10	2389.95	1870.28
Rio Pascua Ante Junta Rio Quetru	-48.15	-73.08	20	1668.09	2137.12
Lago Ohiggins En Villa Ohiggins	-48.51	-72.59	300	752.40	909.18
Candelario Mancilla	-48.87	-72.73	300	850.18	519.25
Rio Punta Eva En Puerto Eden	-49.11	-74.41	10	3607.47	2840.15
El Calafate Aero	-50.26	-72.05	204	433.19	149.60
Lago Dickson	-50.82	-73.11	200	1301.05	1130.96
Lago Paine	-50.84	-72.90	440	1132.83	500.30
Cerro Guido	-50.89	-72.33	230	820.83	312.50
Amalia	-50.95	-73.69	0	4350.81	2801.60
Rio Paine En Parque Nacional 2	-50.96	-72.79	90	1139.24	724.67
Nunatak Grey	-50.97	-73.22	300	1414.56	589.70
Lago Sarmiento	-51.01	-72.71	110	1111.92	352.85
Lago Pehoe	-51.07	-72.99	40	1347.67	868.18
Lago Grey	-51.11	-73.13	50	1397.74	663.07
Glaciar Tindall	-51.11	-73.28	345	1584.05	1200.28
Torres Del Paine	-51.18	-72.96	25	1431.40	750.34
Rio Rincon En Ruta Y-290	-51.31	-72.82	36	1554.36	769.70
Rio Serrano En Desembocadura	-51.33	-73.10	25	1671.86	1227.01

Table S4. Summary of the WRF configuration.

Deleted: 3

	Value
Domain configuration	
Horizontal grid spacing	12.5-km, 2.5-km, and 500-m
Vertical levels	55
Model top pressure	100 hPa
Model physics	
Radiation	RRTMG
Microphysics	Morrison
Cumulus	Kain-Fritsch
Planetary boundary layer	MYNN Level 2.5
Atmospheric surface layer	Monin Obukhov
Land surface	Noah-MP
Top boundary condition	Rayleigh damping
Lateral boundaries	
Forcing	ERA-Interim 0.75ºx0.75º, 6-hourly

I thank the reviewer for the constructive comments and suggestions. My response to the review can be found in the attached document.

R: Referee's comment
A: Author's response
C: Proposed changes in the manuscript

Summary

R: Sauter presents an evaluation of the precipitation magnitude across southern South America. The emphasis is given in the implications to the surface mass balance(SMB) of both Icefields. New data is mainly compared with previous SMB models. Based on the data obtained from an Orographic Precipitation Model, the main conclusions are that Patagonia is not the wettest place on Earth and that the previous SMB overestimates the accumulation. The scientific significance is high regarding the lack of information (and observations) of the actual magnitude of the precipitation on the Patagonian Icefields. The scope of the research is clear and prove (based on the used datasets and assumptions), that higher amount of precipitation previously reported are not sustained by the moisture flux over the region, although this conclusion, of course, will continue to be subject of discussion in the future. The manuscript is within the scope of HESS, it is in general well-written. The reason for the study must be well justified in the Introduction. The Methodology section needs to clarify and add some explanations, as well as some dataset and experiments details used for validation/comparison. The Results/Discussion section needs to be strengthened. I think this paper provides interesting data and results to the glaciological and hydro-climatological communities. In my opinion, it must be considered for publication after solving/clarifying some issues (see Major comments) and a careful revision of the text(see Minor comments).

A: I appreciate very much the overall positive evaluation of the script and will follow the suggestions of the expert in the respective sections. I also agree with the expert's opinion that the discussion about the precipitation in Patagonia is not yet finished and that further relevant studies will be necessary in the future to close the knowledge gap and open issues. I am convinced that this work is a step in the right direction.

Introduction

R: As one of the main topics is the implication of the precipitation on the mass balance on the Icefields, a detailed review of the previous estimations is necessary, considering also the title of the Manuscript. This is barely mentioned, but a comprehensive revision will be helpful for the reader and also will give a strong justification to the present work, mainly related to the fact that besides all the past efforts, still high uncertainties exist in the precipitation magnitude and/or accumulation rate on the Patagonia Icefields.

A: In the present version, only the range of previous mass balance studies with the corresponding literature sources was deliberately mentioned. Most of the literature sources mentioned here summarize the mass balance studies published so far. Since no scientific added value is generated by a new summary, only the previous studies were referred to here. In order to emphasize the importance of the study further I will follow the suggestions of the expert gladly and will work out more precisely the necessity of the study in view of existing work.

C: The last sentences of the first paragraph of the introduction (p2 l8-15) will be revised with respect to existing studies.

R: In this section, it is mentioned the importance of the atmospheric rivers as a source of moisture on Patagonia (first paragraph), but a previous work (Langhamer et al., 2019) indicated that the main source of moisture for the South Patagonian Icefield is the Pacific Ocean between 30◦and 60◦S. Please, clarify this.

A: Atmospheric rivers from the Pacific always lead to a strong increase in water vapour transport and consequently to the strongest precipitation events in Patagonia. These water vapor-rich outbursts occur in the tropical Pacific as a result of geostrophic turbulence. The statement in our paper (Langhamer et al., 2018) that the dominant moisture source in the South Pacific is between 80-160ºW and 30-60ºS does not contradict this statement but confirms the observation. Furthermore, looking at the identified moisture source patterns of Langhamer et al (2018) one can see that this also corresponds to the statistically mean tracks of atmospheric rivers.

C: At the beginning of the introduction (p1 l24-27) I will refer explicitly to the study by Langhamer et al. (2018) and its results.

Soundings

R: It seems that the soundings are used to validate and corrected the WVF from ERA-Interim. Although the information about the WFV trend for both soundings is interesting, it is not used in the analysis. A Figure showing the comparison of the observations with the ERA-Interim data will be useful to understand the bias correction (Page 5, Lines15-20). Please note that the SSMIS data is not mentioned in the Methodology section as a dataset used for comparison.

A: Yes, the radiosondings were used in this study exclusively to evaluate the ERA interim data. A detailed analysis of the trends was not in the spotlight here. Nevertheless, I fully agree with the reviewer regarding the relevance of these data. The WVF time series show very exciting phenomena, such as the influence of atmospheric modes or the presence of decadal signals (water vapor flow) in Punta Arenas while a continuous trend is observed in Puerto Montt. This raises the pressing question which processes can lead to this very different response and to what extent this is related to a changing climate. These exciting questions might open up new perspectives that need to be addressed in detail in follow-up studies and would go beyond the scope of this work.

C: In Figure 2 the time series of the WVF anomaly of the ERA interim were also shown in the first version. For the sake of clarity, the time series were taken out again and the statistical differences (bias, trend, etc.) were presented in the text. If desired, I will add the ERA interim anomalies again in Fig. 2. Many thanks also for the note that the SSMIS dataset was not introduced. I will introduce the dataset accordingly.

Spatial differences

R: It is well established that there are extreme climate gradients on the region, and the results of this work also provide evidence of this, however, in terms of SMB just a mean value is used for each Icefield (NPI and SPI). The author must consider the spatial differences and/or the heterogeneous response of theses glaciers determined by the geodetic method (e.g. Malz et al., 2018; Jaber et al., 2019). Overall, the discussion is related to the glacier shrinkage, despite that, some glaciers show positive (e.g. Pio XI) and stable mass balance.

A: The extreme climate gradients are probably one of the strongest worldwide and probably not only in terms of the drying ratio, as was shown by the reviewer in his relevant study (Bravo et al., 2019). These inevitably lead to a strong west-east differentiation of the surface mass balance and, in interaction with the dynamic effects, to very heterogeneous responses. In our study (Braun et al., 2019) we were able to show by means of TandemX satellite data that the dynamic adjustment of large glaciers plays a decisive role. Evidence has been provided that ice dynamic probably leads to temporary stable mass balances of some glaciers. Unfortunately, such a differentiated analysis is not possible within the approach of this study. This is mainly due to the fact that the SMB is derived from the simplified SMB-accumulation relationship derived from the work of Schaefer et al. (2015) (see Fig. 4). This approach can only be applied to the overall mass balance and is not valid for a differentiated consideration. However, Table 1 can be extended accordingly to emphasize the strong west-east differentiation. Here new columns can be inserted which show the mean precipitation values for individual height zones on the west or east side.

C: I will extend Table 1 and point out again in Section 4 that the approach does not allow differentiation in the mass balance.

Mass balance uncertainty

R: The approach to calculating the mass balance is simple but useful to demonstrate the implication of the overestimation of the accumulation rate. However, it must be mentioned other source of uncertainty on SMB estimations. Recent work indicates that the method chosen to estimate the ratio of solid precipitation is also a source of uncertainty in accumulation estimations (Bravo et al., 2019). This even could lead to lower accumulation rate than those mentioned in the manuscript as the method used is quite simplistic.

A: This is absolutely correct and the other sources of uncertainty have not yet been sufficiently addressed.

C: Other sources of uncertainty, such as uncertainty in the solid-liquid relationship, are explored in more detail in the discussion at the end of Section 3.3.

Limitations and nonlinearities

R: This section presents a comprehensive analysis of the main source of uncertainty, related to the linear nature of the model. This is quite interesting and necessary in a work of this nature, and the last three lines of this section (Page 8, Lines 11-14) is a perfect summary of this section. However, this analysis should be useful if quantification of the uncertainty is given. This quantification could be obtained from the WRF experiment, which also needs to be mentioned in the Methodology section. This section also uses three of a totals of seven Figures to explain the limitations, please check if is really necessary the three Figures.

A: A detailed quantification of the uncertainties can hardly be carried out due to the sparse observations. In section 3.2 (and table S2), the mean deviations of the simulations from the observations (p6 l2-5) were discussed as far as possible.

"…*Comparison with in-situ observations from the Dirección de General de Aguas (DGA, Chile) indicates that the model slightly overestimates precipitation on the leeward side by 0.29±0.37 m yr^{-1}(see Table S2). Greater deviations (1.07±1.30 m yr^{-1}) occur at the stations on the west side which are located at the foot of the Patagonian Icefields. The overestimation is the result of the rapid increase in model terrain elevation and the absence of nonlinear processes in the linear model (see Sec. 3.4*)…"

A comparison with the WRF simulations is not suitable for the quantification of the uncertainty for two main reasons: (i) WRF simulations were only performed for single events to analyse the effect of atmospheric blocking on the precipitation distribution, and (ii) the simulations themselves cannot be considered as 'reality' and are themselves subject to very high uncertainties. For the mentioned reasons, a detailed quantification is only conditionally possible.

The three figures have been chosen so that the limitation of the approach and the nonlinear nature of the processes are evident. Figure 5 shows how often such atmospheric blocking events occur and how often the approach has to be challenged. The subsequent figure shows the underlying processes and theoretical effect on precipitation that may not be familiar to every reader. Figure 6 then finally provides numerical evidence for the effects.

C: If the readability of the article is impaired by the number of figures or the number exceeds the allowable number, I would suggest not to use Figure 5.

Consistency on percentages

R: Please clarify the percentage of overestimation regarding previous works. For instance, it is mentioned in Page 6 Lines 15-16 that the maximum precipitation (11.58 +-0.98 myr-1) represents a reduction of 60% compared to other numerical studies, while in the Conclusions section (Page 8, Lines 21-22) this same value represents a reduction of 30-50%. Please also check the other percentages given.

A: Thank you for pointing that out. This is an error and the correct information should be read ‘up to 60%’.

C: I will check the consistency of the percentages throughout the document and adjust them if necessary.

Minor comments

A: I will review and correct all the comments made by the reviewer.

I thank the reviewer for the constructive comments and suggestions. My response to the review can be found in the attached document.

R: Referee's comment
A: Author's response
C: Proposed changes in the manuscript

General comments

R: Generally I think it is a study which has the potential to make an important contribution to our understanding of precipitation patterns in the study region. However, giving that the results of this study are quite different from previous numerical studies, I am missing are more dedicated search for the reasons of this differences in the discussion section (I am giving some ideas in the specific comments). Furthermore I think that an analysis of the implications of this study for the surface mass balance of the Northern Patagonia Icefield (NPI) would add very much. Here the results could be validated much better against geodetic glacier mass balances since the losses by calving are much better constraint than for SPI (only one tidewater calving glacier on the NPI). Also readability of the manuscript (especially for not climate modelers) could be easily improved. Please find more detailed comments below.

A: Many thanks for the fundamentally positive assessment of the study. I will implement the constructive remarks and comments conscientiously and make the manuscript more accessible to a wider readership. The extension of the study to the NPI would certainly be interesting, but the linear relationship between precipitation and SMB does not necessarily apply to the NPI. Therefore, I would prefer to omit the NPI analysis.

Specific comments

R: Line11: "volume loss of the Patagonian Icefields, for example, contradicts the reported positive surface mass balances" there is no contradiction if the difference can be attributed to calving fluxes (or other mass losses).Example Antarctica: positive SMB, negative overall MB.

A: That's correct.

C: I'll re-write the sentence, for example:

"… The Patagonian Icefields, for example, are one of the largest contributors to sea-level rise outside the polar regions, and robust hydroclimatic projections, in particular estimates of precipitation, are needed to understand and quantify current and future changes. The reported projections of precipitation from numerical modelling studies tend to overestimate those from in-situ determinations and the plausibility of these numbers have never been carefully scrutinised, despite the significance of this topic to our understanding of observed environmental changes. …"

R: Line11-14: Reformulate: you are using a model in this study (and not only a simple physical argument) and get some results. Describe the model briefly: what are the input data and main assumptions.

A/C: I will reformulate the text.

Introduction

R: Line 12/13: up to 30 m w.e. yr -1 are suspected at isolated locations (Lenaerts et al., 2014; Mernild et al., 2017; Schaefer et al., 2013, 2015;Schwikowski et al., 2006). Revise citations! In Schaefer et al., 2013, 2015 no precipitation of up to 30 m w.e. yr^{-1} are suspected (I think only Lenaerts et al., 2014 is mentioning this value!)

A/C: In fact, the figure of 30 m w.e. yr^{-1} was mentioned only by Lenaert and the estimates of the other studies are lower. For this reason the formulation 'up to 30 m' was used and not 'all studies show values of 30 m'. I confess that the formulation can be somewhat confusing and will correct this.

R: Line 29-34: to improve readability, I would recommend to leave the assumption ii) shorter. 1-2 sentences. You can explain the technical details in the method section.

A: In order to increase the readability I will shorten the second assumption slightly.

C: I will move the following sentences to the method part: “This criterion requires a stably stratified atmospheric flow, more precisely given by a positive moist buoyancy frequency. During the study period from2010 to 2016, the condition was fulfilled in more than 99% of all days. … The linearity requirement was met in 82% of the cases (see Sec. 3.4)”.

R: Line 7: Replace “and critically reviewed (Section 3.4) ” by “limitations of the linear precipitation model are discussed in Section 3.4”

A/C: Will be done.

Methodology

R: To improve readability I recommend to divide the methods section in three subsections:
2.1 DR-scaling using a constant precipitation gradient
2.2 DR-scaling using the linear precipitation model
2.3 Examination of non-linearities using the Regional Climate Model WRF (new section)

A/C: In order to make the chapter clearer, I will divide the section into the following subchapters:
2.1 DR-scaling
2.2 Linear orographic model
2.3 Numerical Simulations with the Weather Research and Forecast (WRF) Model

R: p3 l16: “by optimizing (Newton-Raphson algorithm) the vertical precipitation gradient” How does this optimizing work? Describe in one sentence and give a reference for further reading.

A: The Newton-Raphson algorithm is a standard optimization method and in my opinion only needs a corresponding reference.

C: I will add a corresponding reference.

R: p3 l17: “determined from the GPM measurement” : determined : how? Or do you mean taken from? Acronym GPM not explained!

A: The abbreviation was indeed introduced only in the caption of Figure 1 and not in the text.

C: I will introduce the abbreviation ‘GPM’ on p3 l17 and replace ‘determined’ with ‘taken from’.

R: p3 l18/19: “The optimization resulted in a vertical precipitation gradient of 0.00052 m m^{-1} (~0.02% m -1), which represents a slightly smaller lapse rate than previously reported (Schaefer et al., 2013)” In Schaefer et al. a precipitation of 5% per 100m was employed. That is more than double the one you used. You could create another scenario using a lapse rate of 5% per 100m!

A: The numbers mentioned in the text still refer to old simulations and are not correct. The optimized lapse rate is $5.29*10^{-2}$ % m^{-1}, and thus 5.3 % per 100 m.

C: I will change the numbers in the text accordingly.

R: p3 l27: “many processes” : name some (or all)!

A/C: Will be done.

R: p3 l31: “it solves two steady-state advection equations” : show the equations or give reference

A/C: I’ll give the references to the corresponding papers.

R: p3 l32: “conversion from cold water to hydrometeors” : cold water IS a hydrometeor? Do you mean cold vapor?

A/C: The sentence must read as ‘cloud water’ and not ‘cold water’. Will be corrected.

R: p4 l2: “and properties” : properties of what? Which properties do you mean?

A/C: The uniform flow characteristics refer to wind speed, atmospheric stability, scale height etc. (i.e. all assumptions made for this model and explained in the following sentences). Only under these assumptions a linear model can be developed at all. I will present this more clearly.

R: p4 l3: “five parameters” : could explain each parameter in one sentence?

A/C: I will revise the description of the linear model so that the purpose of the parameters is easier to understand.

R: p4 l8: “background precipitation is scaled by a constant” : which range of values does this constant take? What happens if you do not force the model to a fixed drying ratio?

A: Since the model is based on the linear (mountain wave) theory, the precipitation is extended into a background value and a perturbation (orographic part). Here it is assumed that the background value does not vary at all or only very slowly. It must also be considered that the perturbations have no influence on the background value. Thus the orographic precipitation model can only represent the orographic induced part of the precipitation and not the total precipitation. The synoptically induced precipitation must therefore be added. In the study there is no constant value for the background value but is adjusted by the drying ratio (including white noise). So if no background value is added, only the orographic part is obtained, which leads to unrealistic total precipitation.

R: p4 l10: “C_w and N_m are calculated from 6-hourly ERA-Interim fields” how?

A: C_w relates the condensation rate to vertical motion in the atmosphere and can be derived from the ratio of the moist adiabatic and atmospheric lapse rates. The effective moist static stability is approximated from the commonly used equation (Fraser et al., 1973; Smith and Barstad, 2004).

C: I will clarify in the text how these parameters have been derived.

R: p4 l14/15: "produce remarkable similar results" which kind of results? Precipitation fields? You should show that in the results and discussion section!

A: Garreaud et al. (2016) has used the WRF model and the linear model to study the orographic precipitation in coastal Southern Chile. They found similarity and high spatial correlations on longer time scales (not daily) between the two models. The findings cannot be directly applied to the study presented, but indicate that the linear model leads to consistent results under realistic setups.

Results and Discussion

R: p4 l27/28: "Along the coast ..." to which data refers this sentence? ERA-Interim cells located at the coast or measurements in Puerto Montt or Punta Arenas?

A/C: 'Along the coast' refers to the Pacific coast where Puerto Montt is located. I agree, this is confusing and will be re-written.

R: p4 l 29/30 Sentence starting with "There is also clear evidence ..." needs citation. Or are you referring to the data in Puerto Montt?

A/C: The evidence follows from Fig. 2 which provides the basis for the discussion (paragraph) here. I will add another citation to Fig. 2 here.

R: p5 l6 : " The ERA-Interin data ..." : please add these data in Figure 2.

A/C: (see also response to reviewer 1). In Figure 2 the time series of the WVF anomaly of the ERA interim were also shown in the first version. For the sake of clarity, the time series were taken out again and the statistical differences (bias, trend, etc.) were presented in the text. If desired, I will add the ERA interim anomalies again in Fig. 2.

R: p5 l12: "SSMIS data" : explain! Are these reliable data?

A/C: (see also response to reviewee 1). The SSMIS dataset was not introduced at this point, but I will provide more information on the dataset. It is reported that the data is reliable over the ocean but underestimates the vertical integrated water vapor over cold surface such as glaciers.

R: p5 l18: "and corrected accordingly" : this means you multiplied the original ERA-interim WVF by 1.1?

A: Yes, the WVF has been bias corrected with a factor 1.1

R: p5 l22: “Pre-Cordillera region” add (see Figure 1)

A/C: Will be done.

R: p5 l29 “.. values agree with precipitation estimates from discharge measurements “ this statement is not true (see table 1).

A: One would have to say is closer to the estimates from the discharge measurements.

C: I will remove this remark.

R: p5 l32: “windward side” and “leeward slopes” what is the extend of this regions? Can you indicate them in Figure 1 or 3?

A/C: The terms refer to all slopes of the Patagonian Icefields facing to or away from the wind. The west-east differentiation is easy to see in Figure 3.

R: p5 l33: “The spatial pattern on the plateau is consistent ...” how can a precipitation pattern be consistent with elevation change measurements? Explain! How do you define “the plateau” ? Indicate this region in Figure 3!

A/C: The remark by the reviewer is justified because the statement can only valid if hardly any ice dynamic processes take place, which was assumed here for the higher area near the ice divide. This is a very simplistic assumption and not necessarily based on hard facts. But the simulated accumulation patterns are very similar to the observations of the geodetic method. It is clear to me that this statement raises further questions which cannot be answered in the context of this study. I would therefore suggest to discard this sentence.

R: p6 l3: “Greater deviations” better say “higher overestimations”

A/C: Will be implemented accordingly

R: p6 l7: “Shiraiwa et al. is not a presenting simulations but measurements. Please indicate that clearly!

A/C: Ok.

R: p6 l7 : “ The large ensemble spread” : how much is it? You have to show that!

A: The ensemble spread is reflected in the uncertainties of the mean values (see e.g. Table 1).

R: p6 l9-10: “ the responsible mechanisms explaining the significant differences remain unclear.” That’s a very sad statement for a scientific contribution! At least try! Potential candidates are: higher drying ratios or higher precipitation gradients in other studies. You also ran the regional climate model WRF. What drying ratios and precipitation gradients did you get from this simulations? Also different study period could be a candidate.

A: The source of uncertainty in such cases can be very diverse. In addition to the actual errors in the input data, uncertainties in the parameterizations are particularly relevant. Some microphysical parametrisation schemes are more 'grauple-friendly' than others which can lead to strong hyrdometeor formation. In addition, a multitude of parameterization combinations can lead to very different results. Each model setup must therefore be examined individually. Errors in the drying ratio are the direct consequence of inadequate process mapping. The own WRF simulations do not provide any further information since no longer time periods were calculated. For single events the DR can deviate strongly from the long-term mean and the isotope measurements. The sources are manifold and can only be speculative in the context of this study.

C: Even if it is very speculative, I will revise this paragraph and work out possible sources.

R: p6 l26-28: "…, we use the significant linear relation (), between annual precipitation sum and annual SMB derived from data of Schaefer et al. (2015). The relationship is: …

A/C: Will be changed accordingly.

R: p6 l30/31 "...would result in a mean SMB between 0.56±0.45 m w.e. yr -1 (7.82±6.28 km -3 yr -1, extreme scenario) and -0.14±0.39 m w.e. yr -1 (-1.95±5.45 km -3 yr -1, realistic scenario) on theSPI (Fig. 4)

A/C: Will be changed accordingly.

R: p7 l1-2: "… the mean mass loss due to calving ranges between -1.5±0.64 (-20.95±8.94 km -3 yr -1) and -0.8±0.58 m. w.e. yr -1 (-11.18±8.10 km -3 yr -1)" Are these values realistic considering that recently calving fluxes of up to 3.81 km^3w.e. yr-1 for one single glacier were observed during the study period (2015)?
Citation: Bown F, Rivera A, Pętlicki M,Bravo C, Oberreuter J, Moffat C (2019). Recent ice dynamics and mass balance of Jorge Montt Glacier, Southern Patagonia Icefield. Journal of Glaciology 1–13. https://doi.org/ 10.1017/jog.2019.47

A: The values presented here are mean values over the entire period (7 years). Individual events can lead to large mass losses which increase the total mass loss in individual years. The event of 2015 cannot be represented with the approach presented here, since in this study the mean SMB is used together with the geodetic mass balance observations which also represented an integrated value. Any error in the SMB estimate inevitably leads to further uncertainties in the calving fluxes.

C: To remind the reader that such individual events are not considered in this study and that individual years can deviate strongly from the values, I will take up the study of Brown et al. (2019) in the discussion.

R: More results of the WRF simulation should be presented in the results section: which precipitation gradients, total precipitation values of the icefields and drying ratios do you obtain from these simulations?

A: As already mentioned in the previous answers, high-resolution WRF simulations were only calculated for single blocking events. The values derived from a few single events such as precipitation gradients, drying ratio and total precipitation would not be representative.

Conclusions

R: p8 l16: " … simple physical arguments ..." again: you are using a numerical model, not a simple physical argument. Better repeat model essentials.

A: A linear (analytical) model is not a numerical model in a strict sense. A numerical model generally consists of a model conception, a closed physical system of equations which are solved by a numerical solver. A analytical model has a mathematical closed form solution. DR-scaling in turn is a clear scaling approach by scaling precipitation by water vapor flux.

C: I suggest to continue to use the term 'scaling' or 'physical argument' for DR-scaling approach and to use the term 'analytical model' or 'linear model' for the orographic precipitation model.

R: p8 l18: ".. other parameter combinations ..." of the model employed here or generally?

A: The statement refers to the models used here. Since these are linear models, all parameter combinations that lie between the realistic scenario and the extreme scenario must also must lead to precipitation values that lie in between.

R: p8 l20: " … clearly defined assumptions. " add which are: …

A/C: Will be done.

R: p8 l22: Shiraiwa et al.,2002 is NOT a modeling study!!!

A/C: I will make that clear.

R: p8 l30/31: "WVF changes would result in a glacier surface mass gain of about 0.57±0.06 m w.e. per degree warming. TAKE CARE HERE!!! The relationship between precipitation and SMB you derived from the data of Schaefer et al. 2015 will not be valid forever. Percentage of solid precipitation will decrease for higher temperatures!

A/C: I'm fully aware of that. For this reason I will repeat at this point the statement of page 7 line 12 'Ignoring the fact that the solid-liquid ratio changes' and explicitly point out that this trend can only be correct for short periods (including a reference to the work of Bravo et al. (2019)).

R: Line 4 : "While the change in ice masses ..." to which change are you referring to?

A/C: This is a general statement suggesting that the change in ice masses is a very illustrative example of how precipitation uncertainties can affect systems.

Figures

R (Figure 1): I am a bit surprised about the many dots! Can you indicate a list of stations (supplementary material) and indicate to which time span the color coding of the measurements corresponds?

A/C: Yes, I will add a column with the corresponding time periods to Table S2.

R (Figure 2): As indicated before, I would like to see the closest ERA-interim gridpoint data added for each station.
would prefer very much absolute data instead of anomalies!

A/C: See previous comment. I prefer to consider the anomalies to get rid of the seasonality without interfering with the trends. It also helps us to compare the different Puerto Montt with Punta Arenas.

R (Figure 3): Both plots are qualitatively very similar. Could you better compare the linear prec. gradient approach with the numerical model (using the same drying ratio)?

A/C: This is not possible since the WRF simulations are event based simulations (see previous comments).

R (Figure 4): revise caption! The red, green and orange dots are the results of this study! Schaefer et al. (2013), Mernild et al. (2016) are indicated as red circles.

A/C: I will revise the figure caption.

R (Figure 4): I not very necessarily I find. Better add a nice figure about the model validation at weather Stations.

A/C: will remove the figure (see also comment of Reviewer 1).

R (Table 1): Lenearts et al. (2013) are indicating mean precipitation estimates in gigatons. You can calculated specific values from that. Also revise the max values (I think 30 m was obtained at SPI).

A/C: Thank you for pointing that out. I will check it out.

Supplementary material

R: A nice graphical representation of Table S2 should be added to the main part of the manuscript. Results of all scenarios should be validated against station data. Perhaps you could realize two scatterplots: one for the windward side and one for the leeward side? Add observation period to the table (or new table, see comment Figure1!).

A/C: I will extend table S2 with additional columns that indicate the observation period and the results of the extreme scenario and DR scaling. If the scatterplots are meaningful I will gladly add them.